Supporting Information

Machine Metathesis: Thermal and Catalyzed Exchange of Piston Rods in Multicomponent Nanorotor/Nanoslider Ensemble

Amit Ghosh,[a,b] Indrajit Paul,[a,b] Suchismita Saha,[a,b] Thomas Paululat, [a,c] Michael Schmittel*, [a,b]

[a] Center of Micro- and Nanochemistry and Engineering, University of Siegen, Adolf–Reichwein–Str. 2, D-57068 Siegen, Germany. [b] Department Chemistry - Biology, Organische Chemie I. [c] Department Chemistry - Biology, Organische Chemie II.

mail: schmittel@chemie.uni-siegen.de

Table of Contents

1. Synthesis

1.1. General information. All reagents were obtained from commercial suppliers and used without further purification. Technical grade solvents were distilled prior to use. Tetrahydrofuran (THF) was pre-dried over basic alumina and then distilled over potassium. Triethylamine (Et_3N) was distilled from calcium hydride. Melting points were measured on a Büchi SMP-11 instrument. ^{1}H-, ^{13}C-, and ^{1}H-^{1}H-COSY NMR spectra were recorded at 298 K using the deuterated solvent as the lock. The chemical shifts refer to the residual protiated fraction of the solvent ($CHCl_3$: δ_H = 7.26 ppm, δ_C = 77.0 ppm; $CHDCl_2$: δ_H = 5.32 ppm). The following abbreviations were used in ^{1}H NMR assignments to describe splitting patterns (s: singlet, d: doublet, t: triplet, dd: doublet of doublets, ddd: doublet of doublets of doublets, brs: broad singlet, td: triplet of doublets, m: multiplet). Values of coupling constant(s) are reported in Hertz (Hz) and the number of protons is implied. The numbering of carbon atoms is usually not in accordance with IUPAC nomenclature guidelines. UV-vis spectra were measured on a Cary Win 50. Electrospray ionization mass spectra (ESI-MS) were recorded on a Thermo-Quest LCQ Deca instrument. Infrared spectra were recorded using a Perkin Elmer Spectrum-Two FT-IR spectrometer. Column chromatography was performed on silica gel 60 (60−230 mesh). Thin layer chromatography (TLC) was performed using Merck silica gel (60 F254). Compounds **2**,[1] **3**,[2] **6**,[1] **7**[3] and **9**[4] were synthesized according to known or slightly modified procedures. The spectral data of these compounds are in good agreement with those in the literature reports.

1.2. Ligands

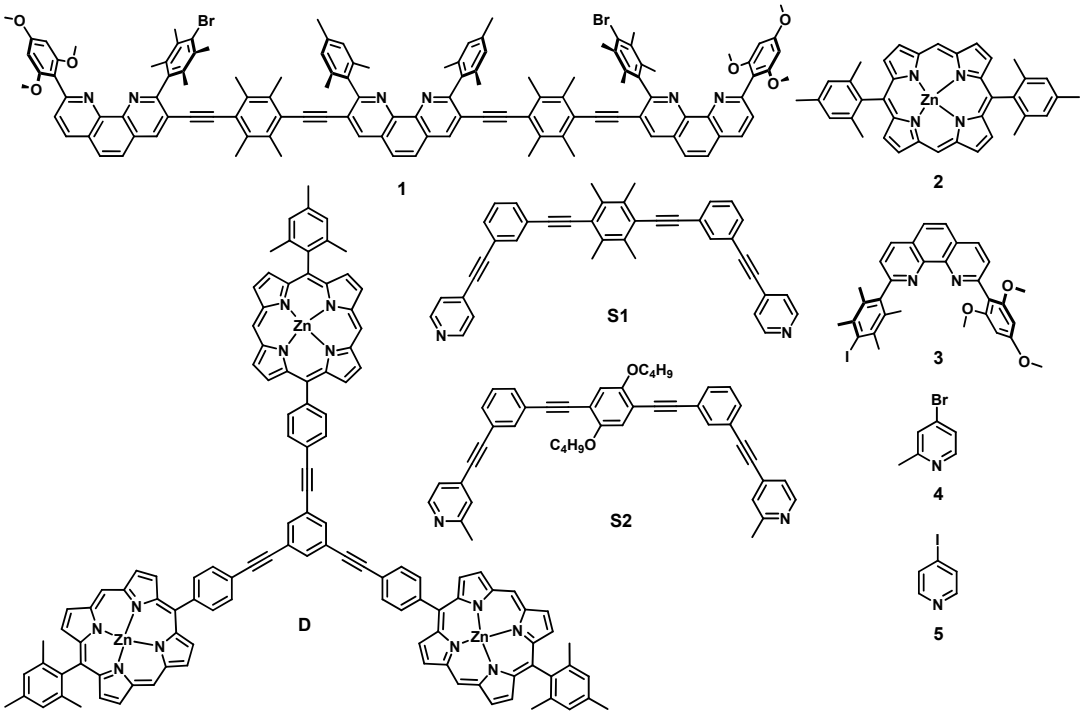

Figure S1. Chemical structures of all ligands used in the present study.

1.3. Synthesis of ligand 1

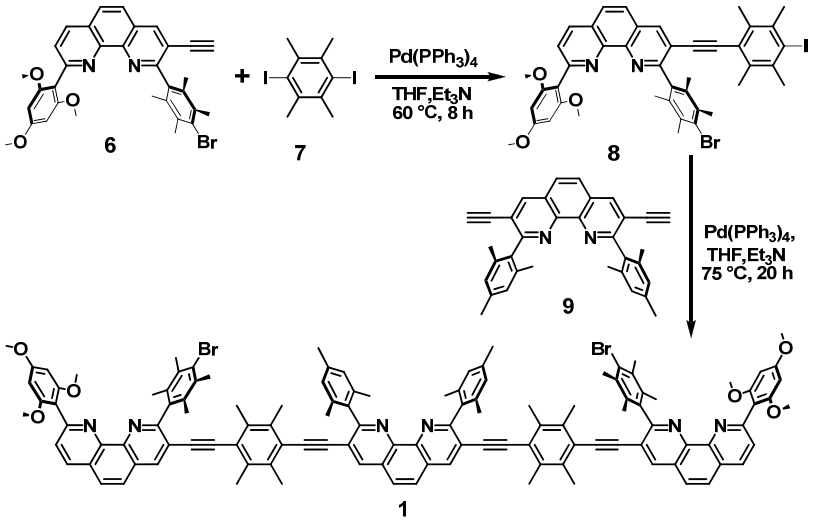

Scheme S1. Multistep synthesis of ligand **1**.

Compound **8**

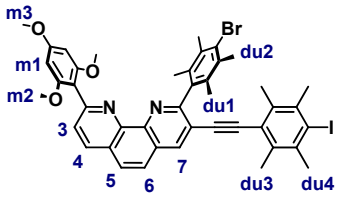

8

In an oven-dried 100-mL sealed tube, a mixture of **6**[1] (150 mg, 258 µmol) and **7**[3] (298 mg, 774 µmol) was dissolved in dry THF (15 mL) and Et_3N (25 mL). After thorough degassing, $Pd(PPh_3)_4$ (30.0 mg, 25.8 µmol) was added and the mixture was refluxed at 60 °C for 8 h for completion of the coupling reaction. The reaction mixture was cooled down to room temperature and the solvents were removed in *vacuo*. The column chromatographic purification (R_f = 0.4, EtOAc : hexane = 2:3) of the crude product on silica gel using 40% EtOAc in hexane provided compound **8** as yellowish solid (150 mg, 179 µmol, 69%) in pure form. **Mp**: > 250 °C. **IR** (KBr): 3424, 2989, 2929, 2835, 2202, 1609, 1586, 1492, 1457, 1435, 1416, 1384, 1335, 1232, 1208, 1188, 1158, 1130, 1068, 1035, 983, 946, 908, 853, 813, 767, 721, 667, 641, 614, 529 cm^{-1}. **^{1}H NMR** ($CDCl_3$, 400 MHz): δ 8.47 (s, 1H, 7-H), 8.22 (d, ^3J = 8.2 Hz, 1H, 4-H), 7.85 (d, ^3J = 8.8 Hz, 1H, 5/6-H), 7.80 (d, ^3J = 8.8 Hz, 1H, 6/5-H), 7.66 (d, ^3J = 8.2 Hz, 1H, 3-H), 6.23 (s, 2H, m1-H), 3.84 (s, 3H, m3-H), 3.73 (s, 6H, m2-H), 2.46 (s, 6H, du2-H), 2.41 (s, 6H, du3-H), 2.17 (s, 6H, du1-H), 2.00 (s, 6H, du4-H) ppm. **^{13}C NMR** ($CDCl_3$, 100 MHz): δ 161.6, 161.5, 159.2, 155.4, 145.9, 144.9, 139.5, 138.7, 137.5, 136.3, 135.2, 133.9, 133.3, 129.2, 127.9, 127.3, 127.0, 126.9, 125.2, 123.1, 120.1, 113.5, 112.9, 94.6, 93.5, 91.8, 56.4, 55.4, 27.6, 20.8, 19.3, 18.4 ppm. **ESI-MS**: *m/z* (%) = 839.9 (100) [(**8**+H)$^+$]. **Elemental analysis** ($C_{43}H_{40}BrIN_2O_3$): Calcd. C, 61.51; H, 4.80; N, 3.34. Found, C, 61.25; H, 4.72; N, 3.40.

Ligand **1**[1]

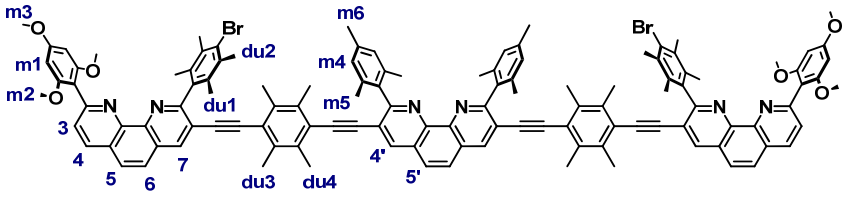

1

Compounds **9** (50.0 mg, 108 µmol) and **8** (181 mg, 216 µmol) were added to a degassed mixture of Et_3N (20 mL) and THF (15 mL). Then, tetrakis(triphenylphosphine)palladium(0) (12.5 mg, 10.8 µmol) was added and the mixture was heated at 75 °C for 20 h. After cooling to room temperature the solvent was evaporated under reduced pressure. The residue was dissolved in DCM (25 mL) and subsequently washed with water (2 × 30 mL). The organic layer was dried over anhydrous $MgSO_4$ and evaporated in *vacuo*. The residue was purified by column chromatography (R_f = 0.4, EtOAc : DCM = 1:4) on silica gel using 20% EtOAc in DCM to yield compound **1** as a yellow solid (110 mg, 58.2 µmol, 54%). **Mp**: > 250 °C. **^{1}H NMR** (CD_2Cl_2, 500 MHz): δ 8.53 (s, 2H, 7-H), 8.52 (s, 2H, 4'-H), 8.27 (d, ^3J = 8.2 Hz, 2H, 4-H), 7.91 (d, ^3J = 8.8 Hz, 2H, 5/6-H), 7.90 (s, 2H, 5'-H), 7.86 (d, ^3J = 8.8 Hz, 2H, 6/5-H), 7.58 (d, ^3J = 8.2 Hz, 2H, 3-H), 6.95 (s, 4H, m4-H), 6.26 (s, 4H, m1-H), 3.87 (s, 6H, m3-H), 3.69 (s, 12H, m2-H), 2.45 (s, 12H, du2-H), 2.35 (s, 6H, m6-H), 2.07 (s, 12H, du1-H), 2.04 (s, 12H, du3-H), 2.03 (s, 12H, m5-H), 2.00 (s, 12H, du4-H) ppm.

1.4. Characterization of ligands D, S1 and S2

Preparation of ligands **D**, **S1** and **S2** was executed as described earlier.[5] Below, we provide their ^{1}H NMR characterization in CD_2Cl_2 for comparison.

Ligand **D**[5]

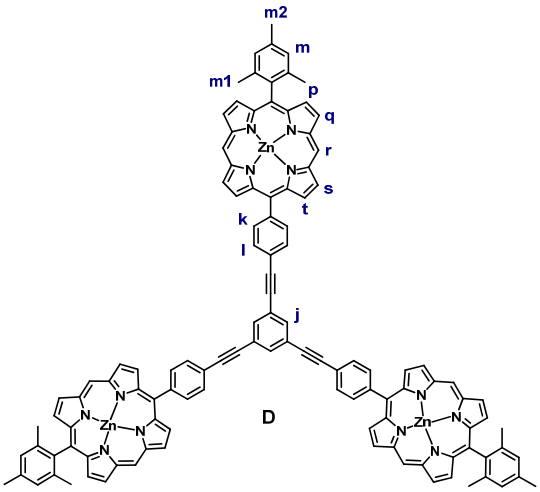

^{1}H NMR (CD_2Cl_2, 400 MHz): δ 10.36 (s, 6H, r-H), 9.54 (d, ^{3}J = 4.4 Hz, 6H, s-H), 9.46 (d, ^{3}J = 4.4 Hz, 6H, q-H), 9.23 (d, ^{3}J = 4.4 Hz, 6H, t-H), 8.98 (d, ^{3}J = 4.4 Hz, 6H, p-H), 8.39 (m, 6H, k-H), 8.15 (m, 6H, l-H), 8.14 (s, 3H, j-H), 7.34 (s, 6H, m-H), 2.67 (s, 9H, m2-H), 1.83 (s, 18H, m1-H) ppm.

Ligand **S1**[5]

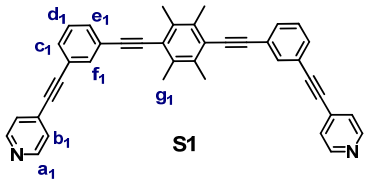

^{1}H NMR (CD_2Cl_2, 400 MHz): δ 8.60 (d, ^{3}J = 6.0 Hz, 4H, a_1-H), 7.77 (td, ^{4}J = 1.6 Hz, ^{5}J = 0.4 Hz, 2H, f_1-H), 7.60 (dt, ^{3}J = 8.0 Hz, ^{4}J = 1.6 Hz, 2H, c_1-H), 7.55 (dt, ^{3}J = 8.0 Hz, ^{4}J = 1.6 Hz, 2H, e_1-H), 7.42 (d, ^{3}J = 6.0 Hz, 4H, b_1-H), 7.38 (t, ^{3}J = 8.0 Hz, 2H, d_1-H), 2.53 (s, 12H, g_1-H) ppm.

Ligand **S2**[5]

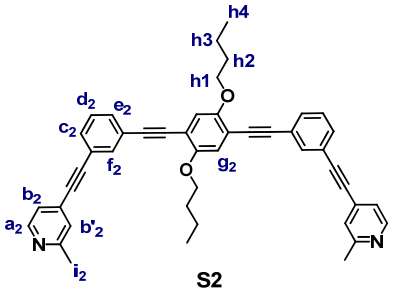

S2

^{1}H NMR (CD_2Cl_2, 400 MHz): δ 8.47 (d, ^3J = 5.2 Hz, 2H, a_2-H), 7.72 (td, ^4J = 1.6 Hz, ^5J = 0.4 Hz, 2H, f_2-H), 7.54 (dt, ^3J = 8.0 Hz, ^4J = 1.6 Hz, 2H, c_2-H), 7.52 (dt, ^3J = 8.0 Hz, ^4J = 1.6 Hz, 2H, e_2-H), 7.40 (t, ^3J = 8.0 Hz, 2H, d_2-H), 7.29 (brs, 2H, b'$_2$-H), 7.21 (dd, ^3J = 5.2 Hz, ^4J = 1.2 Hz, 2H, b_2-H), 7.06 (s, 2H, g_2), 4.06 (t, ^3J = 6.4 Hz, 4H, h1-H), 2.54 (s, 6H, i_2-H), 1.86 (m, 4H, h2-H), 1.60 (m, 4H, h3-H), 1.03 (t, ^3J = 7.6 Hz, 6H, h4-H) ppm.

2. Synthesis and characterization of the complexes

All solid components of the complexes were placed in an NMR tube and dissolved in CD_2Cl_2.

a) Model complex **C1**

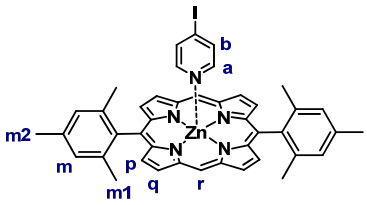

C_1 = [(2)(5)]

In an NMR tube, ligands **2** (1.42 mg, 2.33 µmol) and **5** (0.478 mg, 2.33 µmol) were dissolved in 500 µL of CD_2Cl_2. The NMR spectrum indicated quantitative formation of the model complex **C1** = [(**2**)(**5**)]. **^{1}H NMR** (CD_2Cl_2, 400 MHz): δ 10.14 (s, 2H, r-H), 9.34 (d, ^3J = 4.4 Hz, 4H, q-H), 8.87 (d, ^3J = 4.4 Hz, 4H, p-H), 7.33 (s, 4H, m-H), 6.42 (d, ^3J = 5.4 Hz, 2H, b-H), 4.10 (brs, 2H, a-H), 2.66 (s, 6H, m2-H), 1.80 (s, 12H, m1-H) ppm.

b) Model complex **C2**

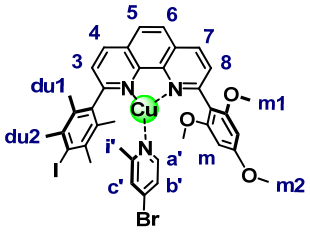

C2 = [Cu(3)(4)]$^+$

In an NMR tube, $[Cu(CH_3CN)_4]PF_6$ (0.868 mg, 2.33 µmol), ligands **3** (1.41 mg, 2.33 µmol) and **4** (0.401 mg, 2.33 µmol) were dissolved in 500 µL of CD_2Cl_2. Yield by NMR: quantitative. **^{1}H NMR** (CD_2Cl_2, 400 MHz): δ 8.68 (d, ^3J = 8.4 Hz, 1H, 8-H), 8.59 (d, ^3J = 8.4 Hz, 1H, 7-H), 8.13 (s, 2H, 5 + 6-H), 7.96 (d, ^3J = 8.2 Hz, 1H, 4-H), 7.87 (d, ^3J = 8.2 Hz, 1H, 3-H), 7.55 (d, ^3J = 6.0 Hz, 1H, a'-H), 7.35 (d, ^4J = 2.0 Hz, 1H, c'-H), 7.22 (dd, ^3J = 6.0 Hz, ^4J = 2.0 Hz, 1H, b'-H), 6.01 (s, 2H, m-H), 3.75 (s, 3H, m2-H), 3.61 (s, 6H, m1-H), 2.37 (s, 6H, du2-H), 2.07 (s, 3H, i'-H), 1.95 (s, 6H, du1-H) ppm**. ESI-MS**: *m/z* (%) = 839.7 (100) [[Cu(**3**)(**4**)]$^+$].

c) Model complex **C3**

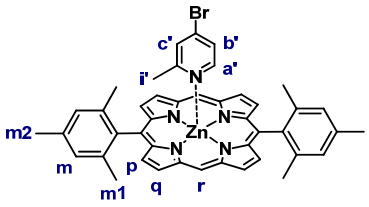

C3 = [(2)(4)]

In an NMR tube, ligands **2** (0.868 mg, 2.33 µmol) and **4** (0.401 mg, 2.33 µmol) were dissolved in 500 µL of CD_2Cl_2. The NMR spectrum indicated clean formation of the model complex **C3** = [(**2**)(**4**)]. **^{1}H NMR** (CD_2Cl_2, 400 MHz): δ 10.19 (s, 2H, r-H), 9.36 (d, ^3J = 4.4 Hz, 4H, q-H), 8.88 (d, ^3J = 4.4 Hz, 4H, p-H), 7.33 (s, 4H, m-H), 6.96 (brs, 1H, c'-H), 6.88 (dd, ^3J = 5.4 Hz, ^4J = 1.4 Hz, 1H, b'-H), 6.82 (d, ^3J = 5.4 Hz, 1H, a'-H), 2.66 (s, 6H, m2-H), 1.80 (s, 12H, m1-H), 1.57 (s, 3H, i'-H) ppm.

d) Model complex **C4**

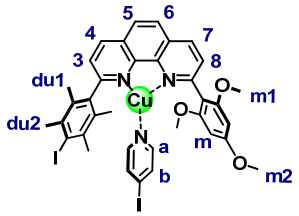

C4 = [Cu(3)(5)]$^+$

In an NMR tube, ligands **3** (1.41 mg, 2.33 µmol) and **5** (0.478 mg, 2.33 µmol) as well as $[Cu(CH_3CN)_4]PF_6$ (0.422 mg, 2.33 µmol) were dissolved in 500 µL of CD_2Cl_2. Yield by NMR: quantitative. **^{1}H NMR** (CD_2Cl_2, 400 MHz): δ 8.67 (d, ^3J = 8.4 Hz, 1H, 8-H), 8.58 (d, ^3J = 8.4 Hz, 1H, 7-H), 8.12 (s, 2H, 5 + 6-H), 7.98 (d, ^3J = 8.2 Hz, 1H, 4-H), 7.86 (d, ^3J = 8.2 Hz, 1H, 3-H), 7.58 (brs, 2H, a-H), 7.04 (brs, 2H, b-H), 6.13 (s, 2H, m-H), 3.83 (s, 3H, m2-H), 3.63 (s, 6H, m1-H), 2.46 (s, 6H, du2-H), 1.96 (s, 6H, du1-H) ppm. **ESI-MS**: *m/z* (%) = 871.7 (100) [[Cu(**3**)(**5**)]$^+$].

e) Nanorotor **R1**

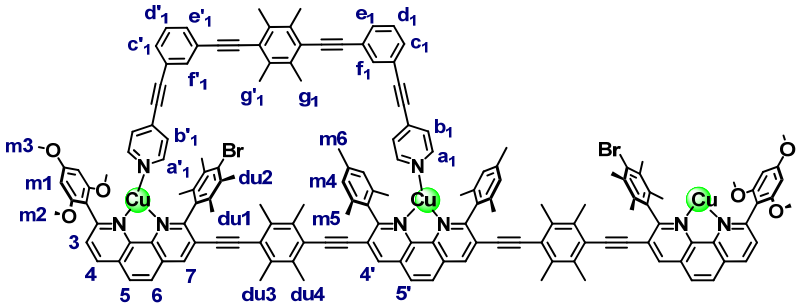

In an NMR tube, $[Cu(CH_3CN)_4]PF_6$ (0.711 mg, 1.91 µmol), stator **1** (1.20 mg, 0.636 µmol) and arm **S1** (0.341 mg, 0.636 µmol) were dissolved in 500 µL of CD_2Cl_2. The NMR spectrum indicated quantitative formation of the nanorotor $[Cu_3(\mathbf{S1})(\mathbf{1})]^{3+}$. **Mp**: > 250 °C; **IR** (KBr): = 3050, 2923, 2918, 2211, 2196, 1608, 1593, 1582, 1569, 1537, 1489, 1478, 1412, 1404, 1333, 1222, 1153, 1124, 1033, 1014, 985, 946, 907, 844, 810, 779, 692, 645, 612, 527 cm^{-1}; ^1H **NMR** (600 MHz, CD_2Cl_2): δ 8.85 (s, 2H, 7-H), 8.81 (s, 2H, 4'-H), 8.57 (d, ^3J = 8.4 Hz, 2H, 4-H), 8.18 (s, 2H, 5'-H), 8.13 (d, ^3J = 9.0 Hz, 2H, 5/6-H), 8.09 (d, ^3J = 9.0 Hz, 2H, 6/5-H), 7.97 (d, ^3J = 8.4 Hz, 2H, 3-H), 7.84 (t, ^4J = 1.2 Hz, 2H, f_1-,f'_1-H), 7.64 (dt, ^3J = 6.0 Hz, $^4J_1$ = 1.2 Hz, 2H, e_1-,e'_1-H), 7.57 (dt, ^3J = 6.0 Hz, $^4J_1$ = 1.2 Hz, 2H, c_1-,c'_1-H), 7.47 (t, ^3J = 6.0 Hz, 2H, d_1-,d'_1-H), 7.39 (brs, 4H, a_1-,a'_1-H), 7.19 (d, ^3J = 6.1 Hz, 4H, b_1-,b'_1-H), 6.99 (s, 4H, m4-H), 6.20 (s, 4H, m1-H), 3.86 (s, 6H, m3-H), 3.69 (s, 12H, m2-H), 2.57 (s, 12H, du2-H), 2.42 (s, 12H, g_1/g'_1-H), 2.41 (s, 6H, m6-H), 2.06 (s, 12H, du1-H), 2.05 (s, 12H, du3-H), 2.03 (s, 12H, m5-H), 1.99 (s, 12H, du4-H) ppm; **ESI-MS**: *m/z* (%) = 871.5 (100) $[[Cu_3(\mathbf{S1})(\mathbf{1})]^{3+}]$; **Elemental analysis** ($C_{158}H_{134}Br_2Cu_3N_8O_6$•$4.5CH_2Cl_2$): Calcd. C, 65.64; H, 4.85; N, 3.77. Found, C, 65.65; H, 4.48; N, 3.82.

f) Nanorotor **R2**

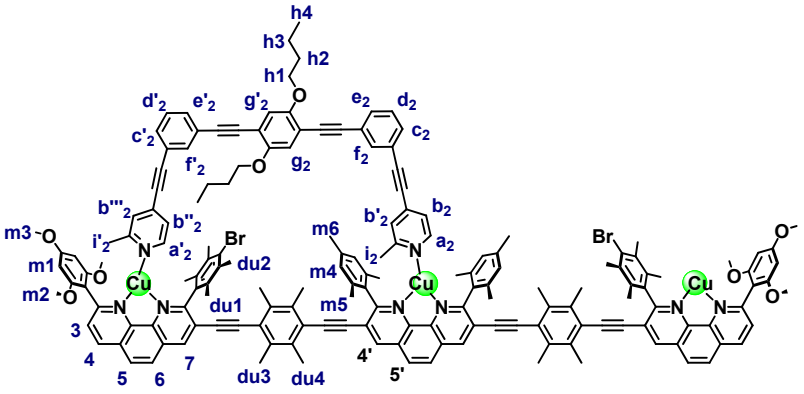

In an NMR tube, $[Cu(CH_3CN)_4]PF_6$ (0.711 mg, 1.91 µmol), stator **1** (1.20 mg, 0.636 µmol) and arm **S2** (0.415 mg, 0.636 µmol) were dissolved in 500 µL of CD_2Cl_2. The NMR spectrum indicated quantitative formation of the nanorotor $[Cu_3(\mathbf{S2})(\mathbf{1})]^{3+}$. **Mp**: > 250 °C; **IR** (KBr): = 2953, 2923, 2118, 2867, 2211, 2196, 1608, 1599, 1582, 1569, 1536, 1503, 1489, 1454, 1413, 1334, 1221, 1203, 1154, 1130, 1032, 980, 946, 908, 844, 810, 750, 698, 645, 610, 530 cm^{-1}; **^{1}H NMR** (600 MHz, CD_2Cl_2): δ 8.84 (s, 2H, 7-H), 8.80 (s, 2H, 4'-H), 8.56 (d, ^3J = 8.4 Hz, 2H, 4-H), 8.17 (s, 2H, 5'-H), 8.13 (d, ^3J = 9.0 Hz, 2H, 5/6-H), 8.09 (d, ^3J = 9.0 Hz, 2H, 6/5-H), 7.96 (d, ^3J = 8.4 Hz, 2H, 3-H), 7.79 (t, ^4J = 1.2 Hz, 2H, f_2-,f'_2-H), 7.58 (dt, ^3J = 6.0 Hz, $^4J_1$ = 1.2 Hz, 2H, e_2-,e'_2-H), 7.54 (dt, ^3J = 6.0 Hz, $^4J_1$ = 1.2 Hz, 2H, c_2-,c'_2-H), 7.45 (t, $^3J_1$ = 6.0 Hz, 2H, d_2-,d'_2-H), 7.45 (brs, 2H, a_2-,a'_2-H), 7.19 (brs, 2H, b'_2-,b'''_2-H), 7.11 (brs, 2H, b_2-,b''_2-H), 7.09 (s, 2H, g_2-,g'_2-H), 6.79 (s, 4H, m4-H), 6.16 (s, 4H, m1-H), 4.10 (t, ^3J = 6.8 Hz, 4H, h1-H), 3.82 (s, 6H, m3-H), 3.68 (s, 12H, m2-H), 2.38 (s, 12H, du2-H), 2.22 (s, 6H, m6-H), 2.04 (s, 12H, du1-H), 2.03 (s, 12H, du3-H), 2.02 (s, 12H, m5-H), 2.00 (s, 6H, i_2-,i'_2-H), 1.98 (s, 12H, du4-H), 1.88 (m, 4H, h2-H), 1.61 (m, 4H, h3-H), 1.05 (t, ^3J = 7.6 Hz, 6H, h4-H) ppm; **ESI-MS**: *m/z* (%) = 910.9 (100) $[[Cu_3(\mathbf{S2})(\mathbf{1})]^{3+}]$; **Elemental analysis** ($C_{164}H_{146}Br_2Cu_3N_8O_8$•$7.5CH_2Cl_2$): Calcd. C, 61.59; H, 4.85; N, 3.35. Found, C, 61.24; H, 4.73; N, 3.40.

g) slider-on-deck **DS1**[5]

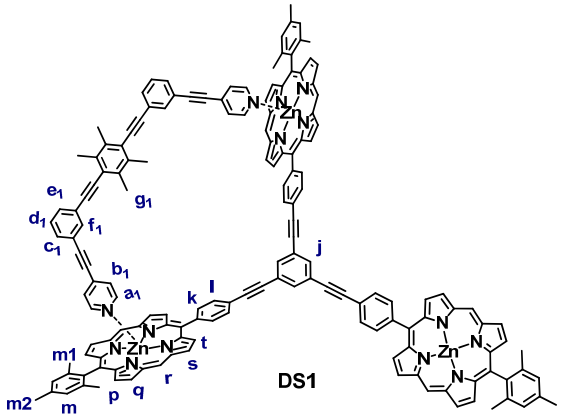

In an NMR tube, arm **S1** (0.435 mg, 0.816 µmol) and deck **D** (1.50 mg, 0.816 µmol) were dissolved in 500 µL of CD_2Cl_2. The NMR spectrum suggested full conversion. **^{1}H NMR** (400 MHz, CD_2Cl_2): δ 10.27 (s, 6H, r-H), 9.48 (d, ^3J = 4.4 Hz, 6H, s-H), 9.40 (d, ^3J = 4.4 Hz, 6H, q-H), 9.20 (d, ^3J = 4.4 Hz, 6H, t-H), 8.94 (d, ^3J = 4.4 Hz, 6H, p-H), 8.40 (m, 6H, k-H), 8.14 (m, 6H, l-H), 8.14 (s, 3H, j-H), 7.36 (s, 6H, m-H), 7.32 (d, ^3J = 6.0 Hz, 2H, c_1-H), 7.23 (brs, 2H, f_1-H), 7.12 (t, ^3J = 7.6 Hz, 2H, d_1-H), 7.00 (d, ^3J = 6.0 Hz, 2H, e_1-H), 5.45 (d, ^3J = 6.0 Hz, 4H, b_1-H) 2.67 (s, 9H, m2-H), 2.31 (s, 12H, g_1-H), 2.22 (d, ^3J = 6.0, 4H, a_1-H), 1.84 (s, 18H, m1-H) ppm.

h) slider-on-deck **DS2**[5]

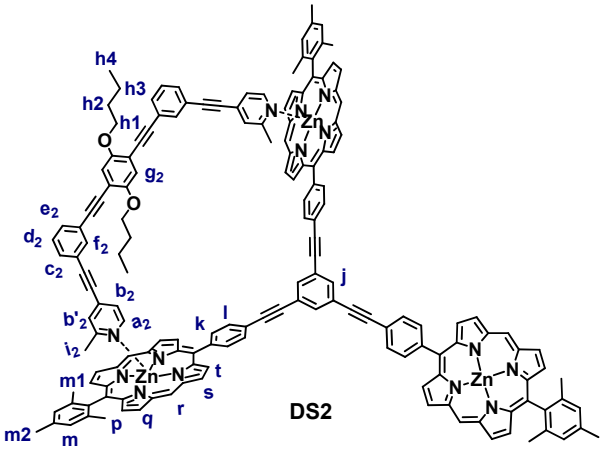

In an NMR tube, arm **S2** (0.533 mg, 0.816 µmol) and deck **D** (1.50 mg, 0.816 µmol) were dissolved in 500 µL of CD_2Cl_2. The NMR spectrum suggested full conversion. **^{1}H NMR** (400 MHz, CD_2Cl_2): δ 10.29 (s, 6H, r-H), 9.49 (d, ^3J = 4.4 Hz, 6H, s-H), 9.41 (d, ^3J = 4.4 Hz, 6H, q-H), 9.20 (d, ^3J = 4.4 Hz, 6H, t-H), 8.94 (d, ^3J = 4.4 Hz, 6H, p-H), 8.38 (m, 6H, k-H), 8.14 (m, 6H, l-H), 8.14 (s, 3H, j-H), 7.39 (m, 2H, c_2, f_2-H), 7.35 (s, 6H, m-H), 7.22 (m, 2H, d_2, e_2-H), 6.91 (s, 2H, g_2-H), 6.05 (brs, 2H, b'$_2$-H), 5.98 (s, 2H, b_2-H), 4.01 (s, 2H, a_2-H), 3.93 (t, ^3J = 6.4 Hz, 4H, h1-H), 2.67 (s, 9H, m2-H), 1.83 (s, 18H, m1-H), 1.72 (m, 4H, h2-H), 1.47 (m, 4H, h3-H), 0.90 (t, ^3J = 7.6 Hz, 6H, h4-H), –0.30 (s, 6H, i-H) ppm.

3. Model study

Self-sorting was tested by mixing **2**, **3**, **4**, **5** and $[Cu(CH_3CN)_4]PF_6$ (2.33 μmol) in a molar ratio of 1:1:1:1:1 in CD_2Cl_2. The subsequently measured ^1H NMR spectrum was compared with those of the individual complexes. Complexes **C4** = $[Cu(\mathbf{3})(\mathbf{5})]^+$ and **C3** = $[(\mathbf{2})(\mathbf{4})]$ were prepared separately in CD_2Cl_2 at 298 K. Mixing of these two complexes using the same conditions affords the more stable complex mixture **C2** = $[Cu(\mathbf{3})(\mathbf{4})]^+$ and **C1** = $[(\mathbf{2})(\mathbf{5})]$.

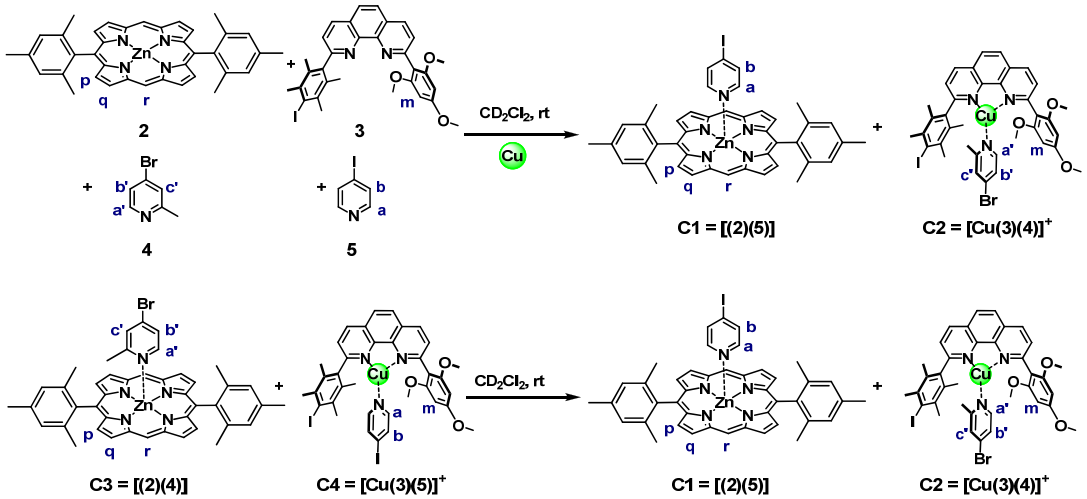

Scheme S2. A two fold quantitative self-sorting studies with ligand **2**, **3**, **4**, **5** and $[Cu(CH_3CN)_4]PF_6$.

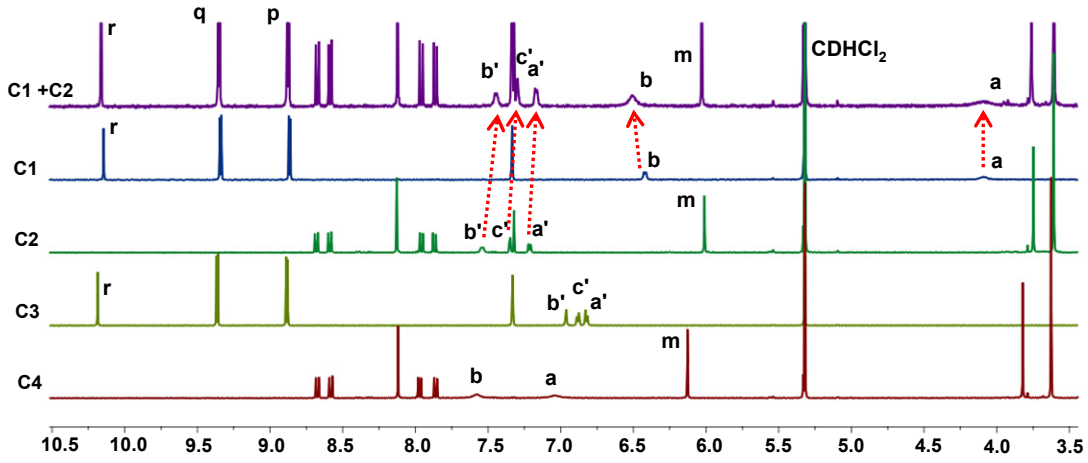

Figure S2. Comparison of ^1H NMR spectra (CD_2Cl_2, 400 MHz) of individual model complexes **C4**, **C3**, **C2**, **C1** and final self-sorted system.

4. NMR spectra: ^{1}H, ^{13}C, ^{1}H-^{1}H COSY

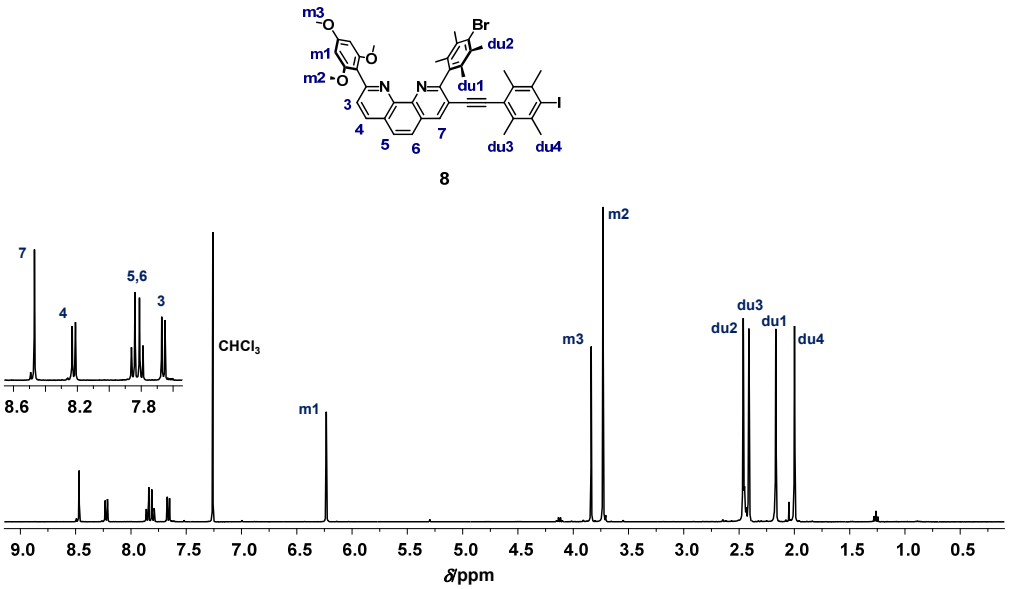

Figure S3. ^{1}H NMR spectrum ($CDCl_3$, 400 MHz) of compound **8**.

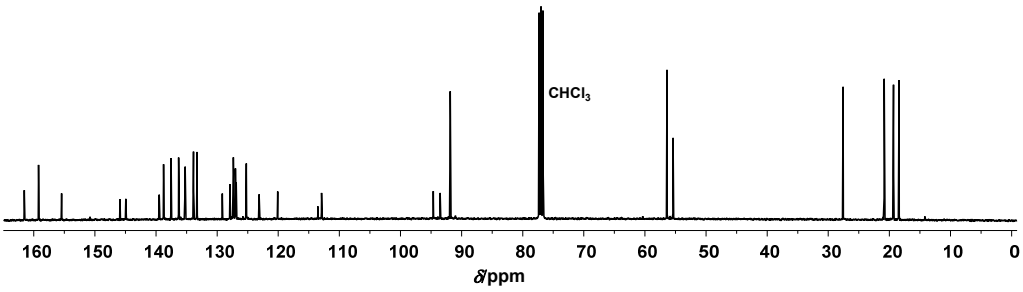

Figure S4. ^{13}C NMR spectrum ($CDCl_3$, 100 MHz) of compound **8**.

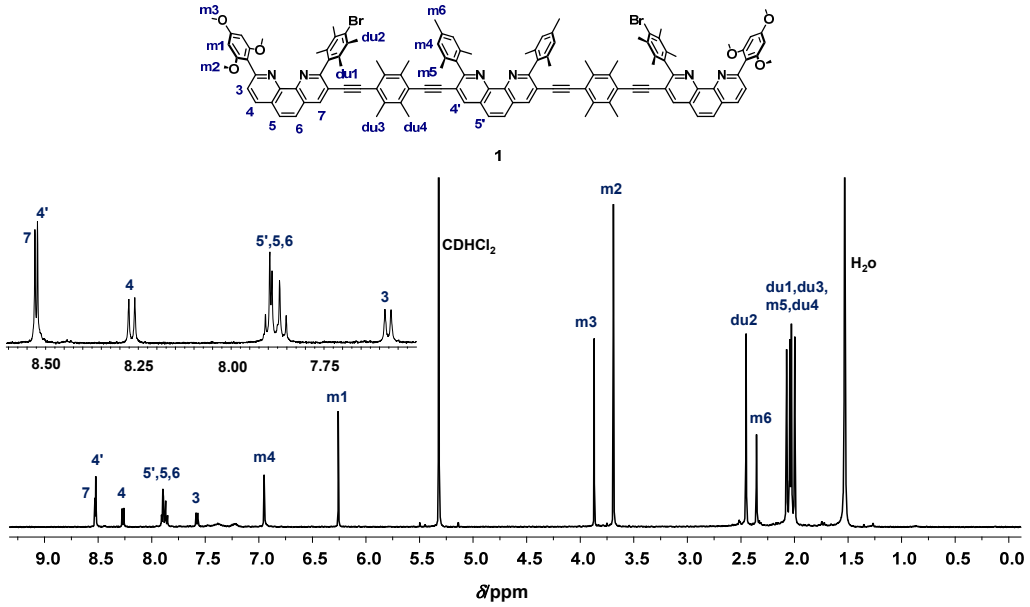

Figure S5. ^{1}H NMR spectrum (CD_2Cl_2, 500 MHz) of ligand **1**.

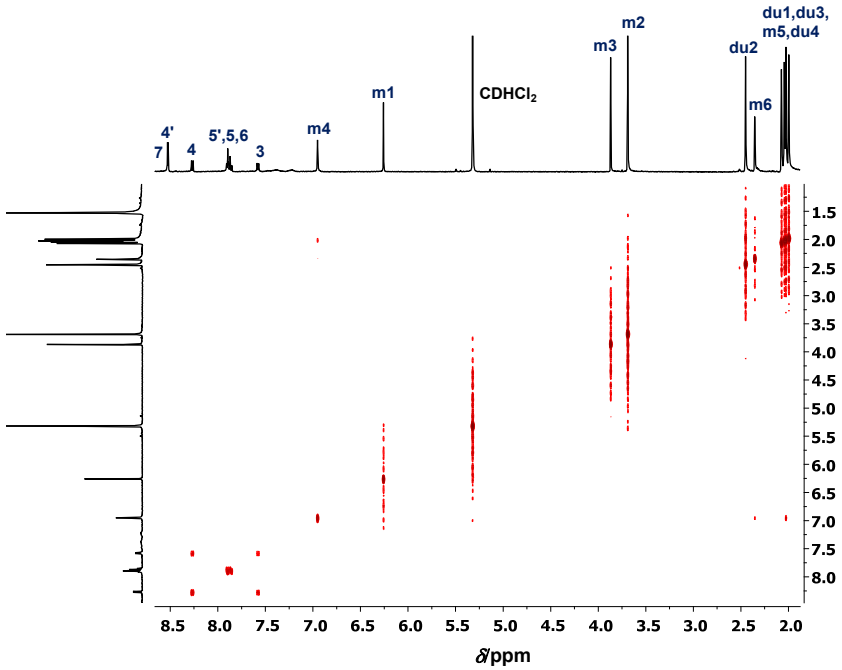

Figure S6. ^{1}H-^{1}H COSY NMR spectrum (CD_2Cl_2, 500 MHz) of ligand **1**.

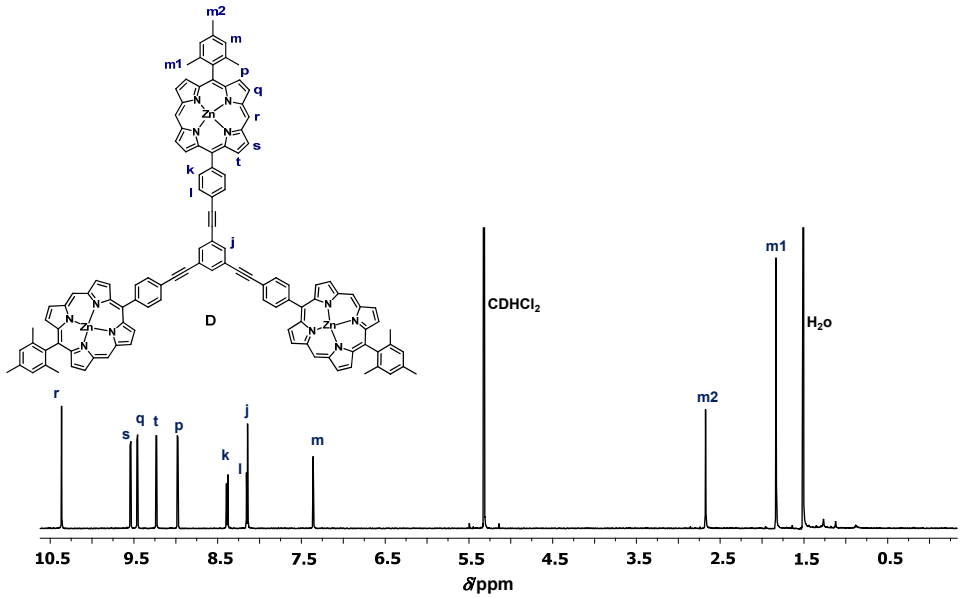

Figure S7. ^{1}H NMR spectrum (CD_2Cl_2, 400 MHz) of ligand **D.**

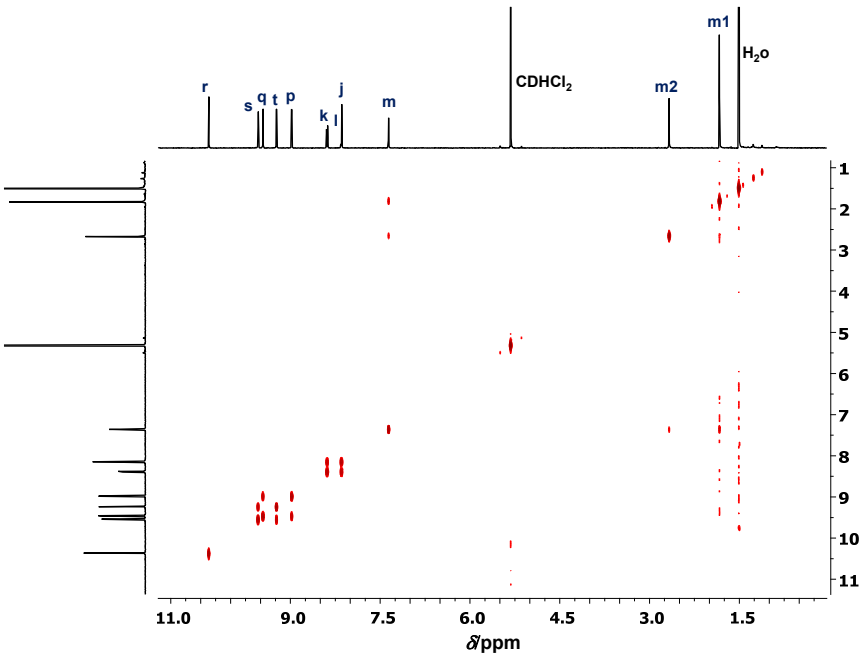

Figure S8. ^{1}H-^{1}H COSY NMR spectrum (CD_2Cl_2, 400 MHz) of ligand **D**.

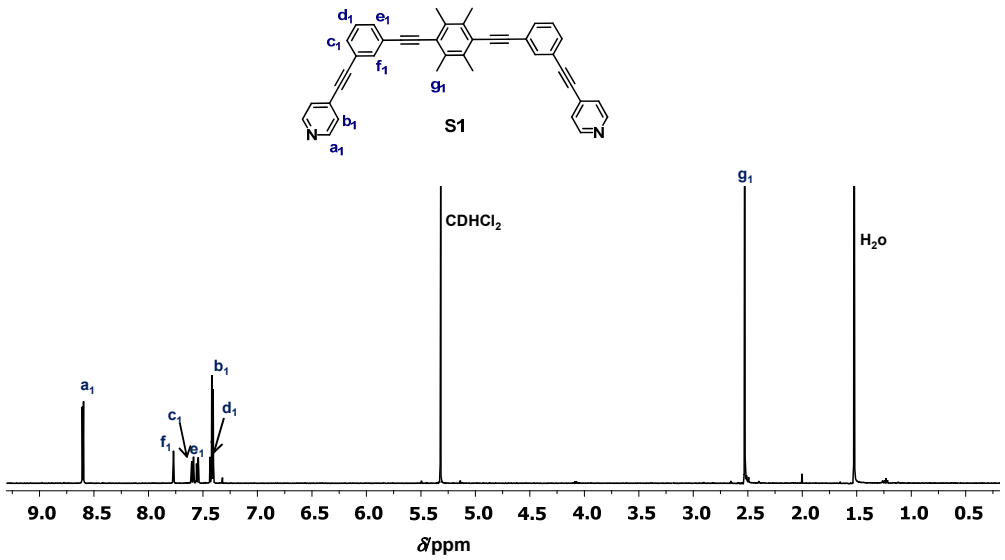

Figure S9. ^{1}H NMR spectrum (CD_2Cl_2, 400 MHz) of ligand **S1.**

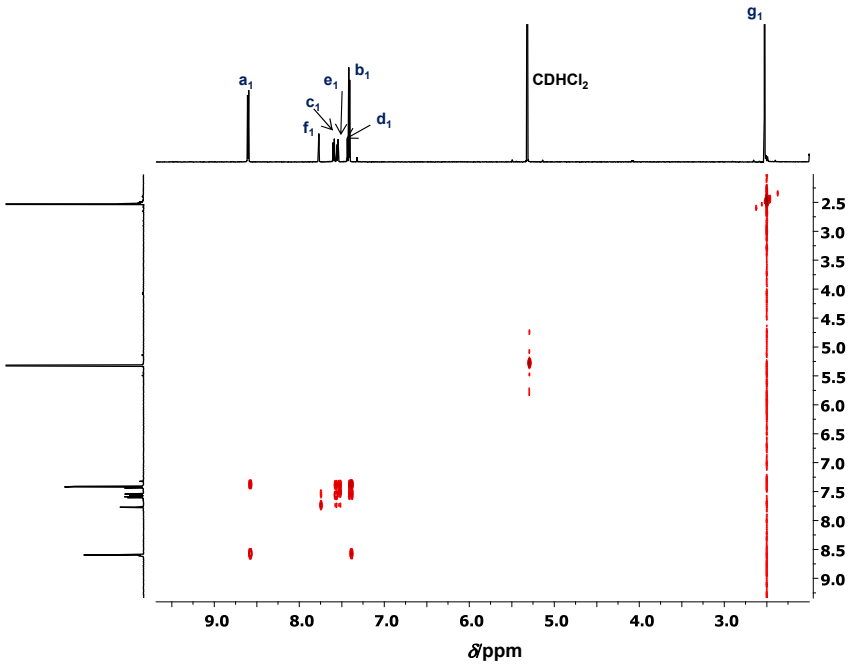

Figure S10. ^{1}H-^{1}H COSY NMR spectrum (CD_2Cl_2, 400 MHz) of ligand **S1**.

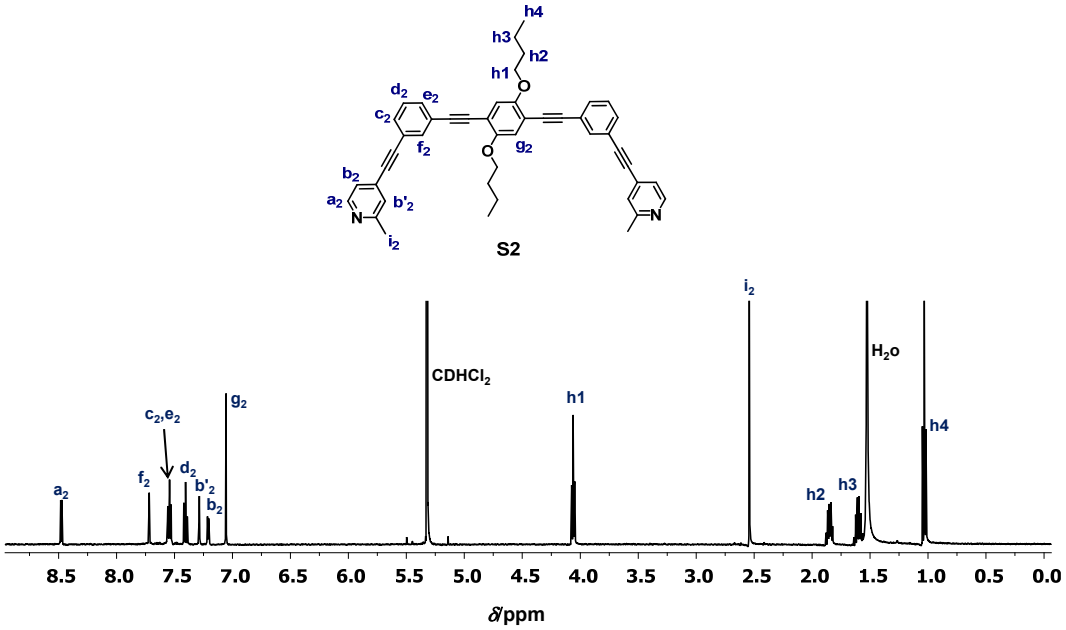

Figure S11. ^{1}H NMR spectrum (CD_2Cl_2, 400 MHz) of ligand **S2**.

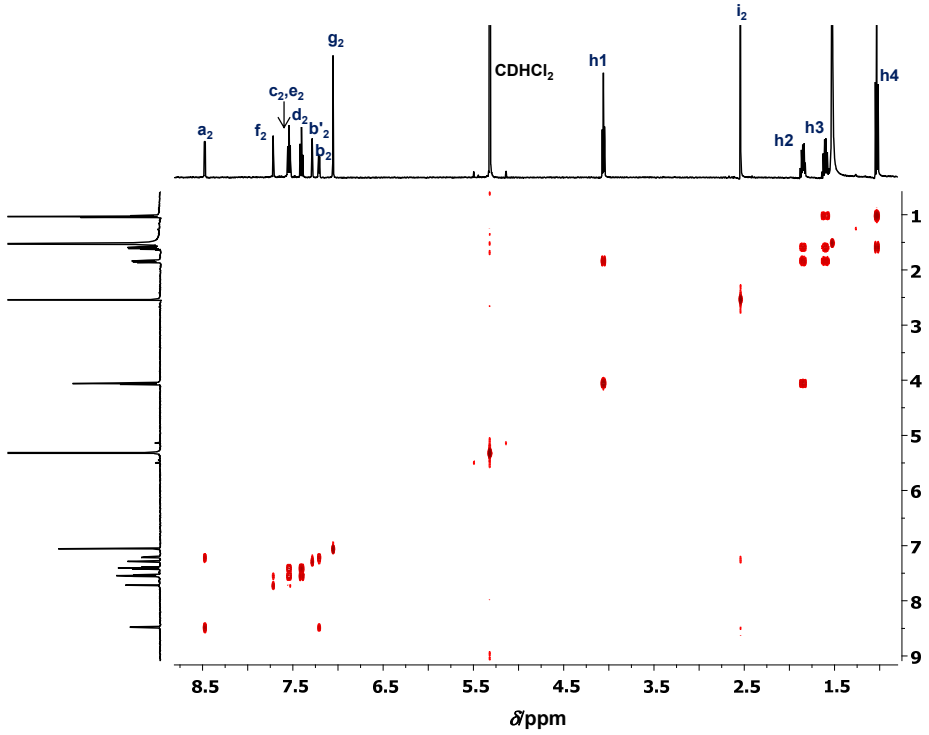

Figure S12. ^{1}H-^{1}H COSY NMR spectrum (CD_2Cl_2, 400 MHz) of ligand **S2**.

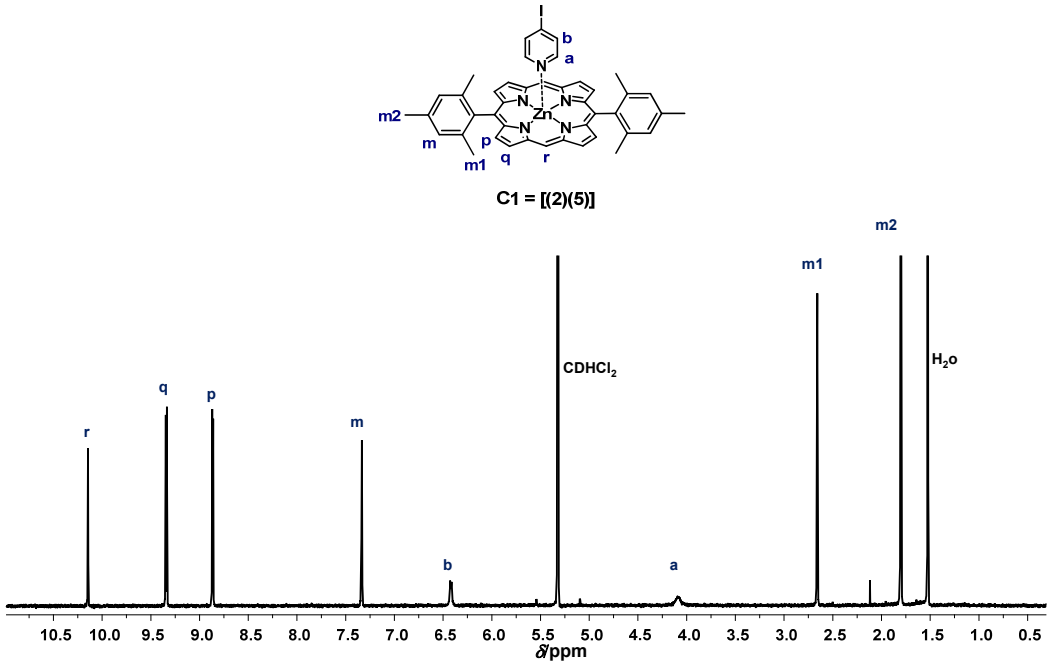

Figure S13. ^{1}H NMR spectrum (CD_2Cl_2, 400 MHz) of complex **C1**.

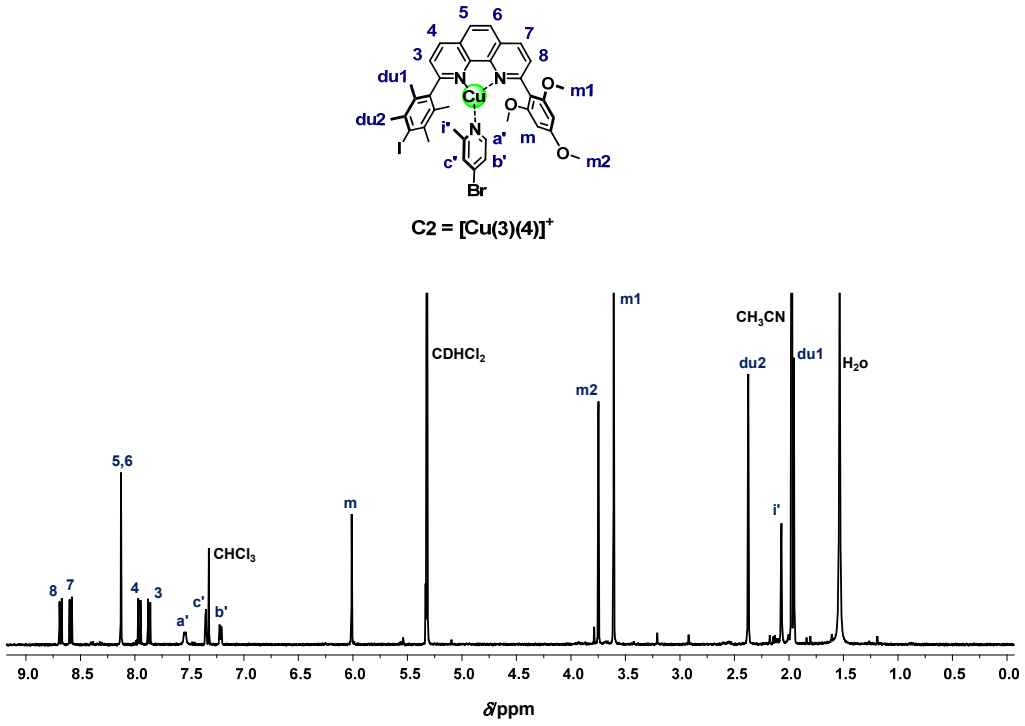

Figure S14. ^{1}H NMR spectrum (CD_2Cl_2, 400 MHz) of complex **C2**.

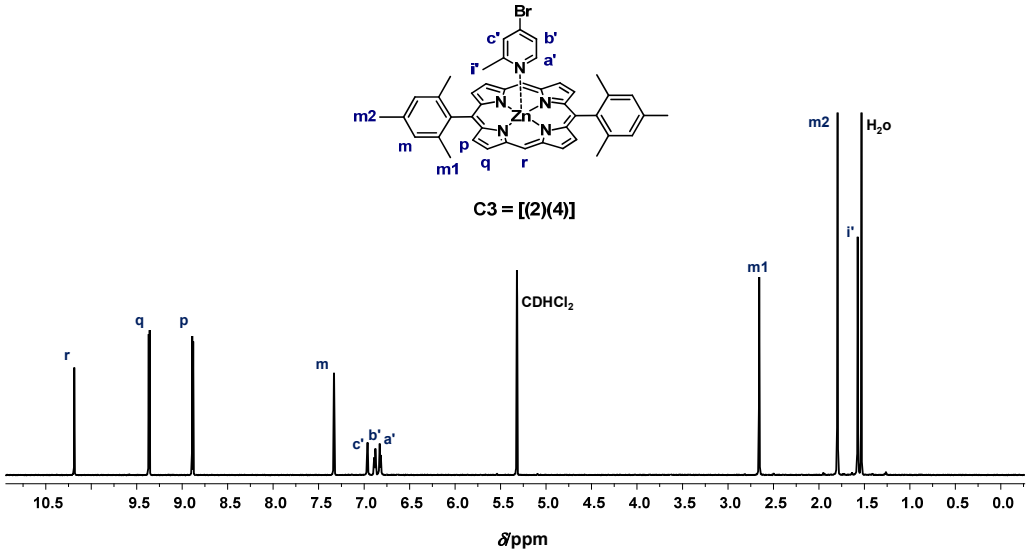

Figure S15. ^{1}H NMR spectrum (CD_2Cl_2, 400 MHz) of complex **C3**.

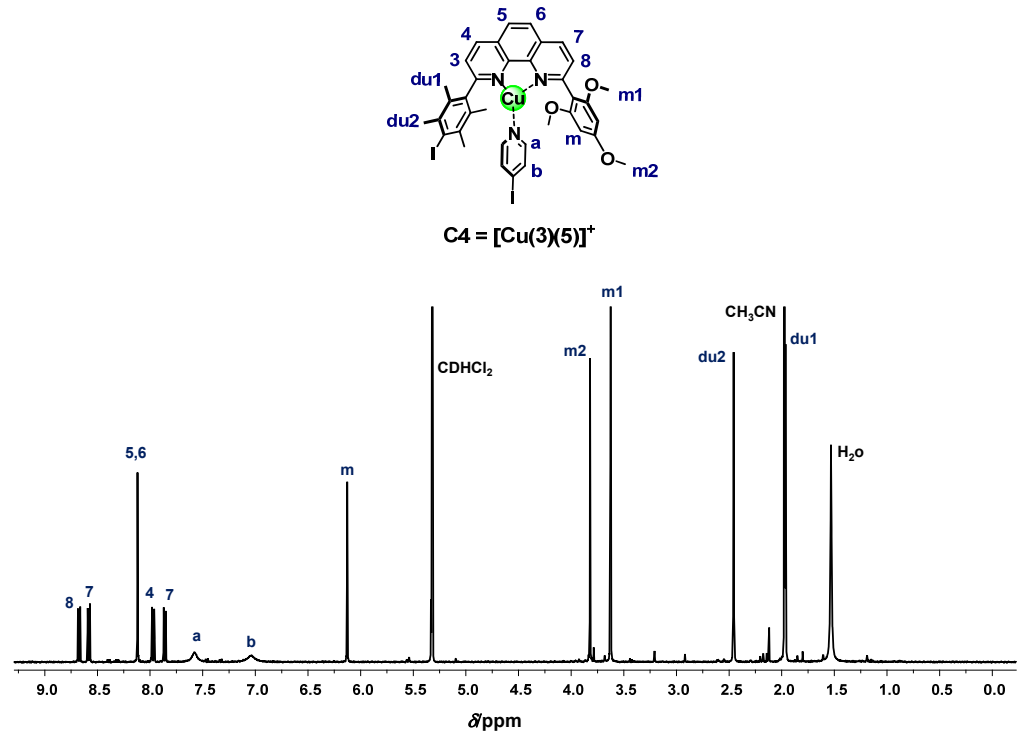

Figure S16. ^{1}H NMR spectrum (CD_2Cl_2, 400 MHz) of complex **C4**.

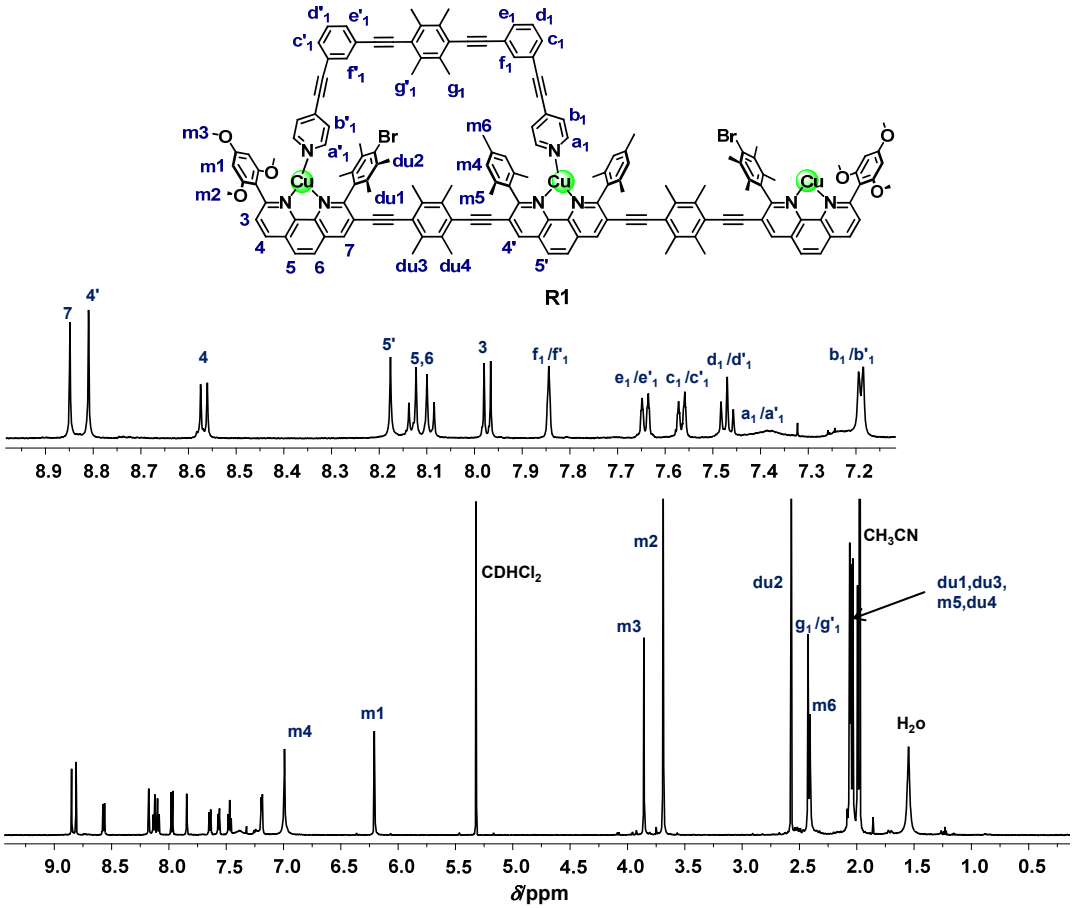

Figure S17. ^{1}H NMR spectrum (CD_2Cl_2, 600 MHz) of nanorotor **R1.**

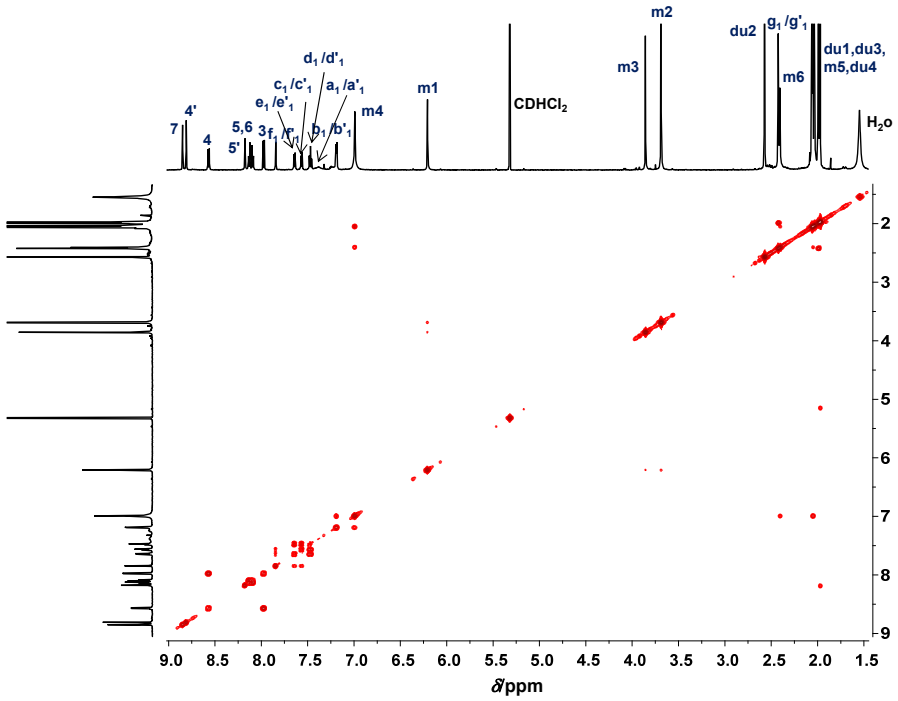

Figure S18. ^{1}H-^{1}H COSY NMR spectrum (CD_2Cl_2, 400 MHz) of nanorotor **R1**.

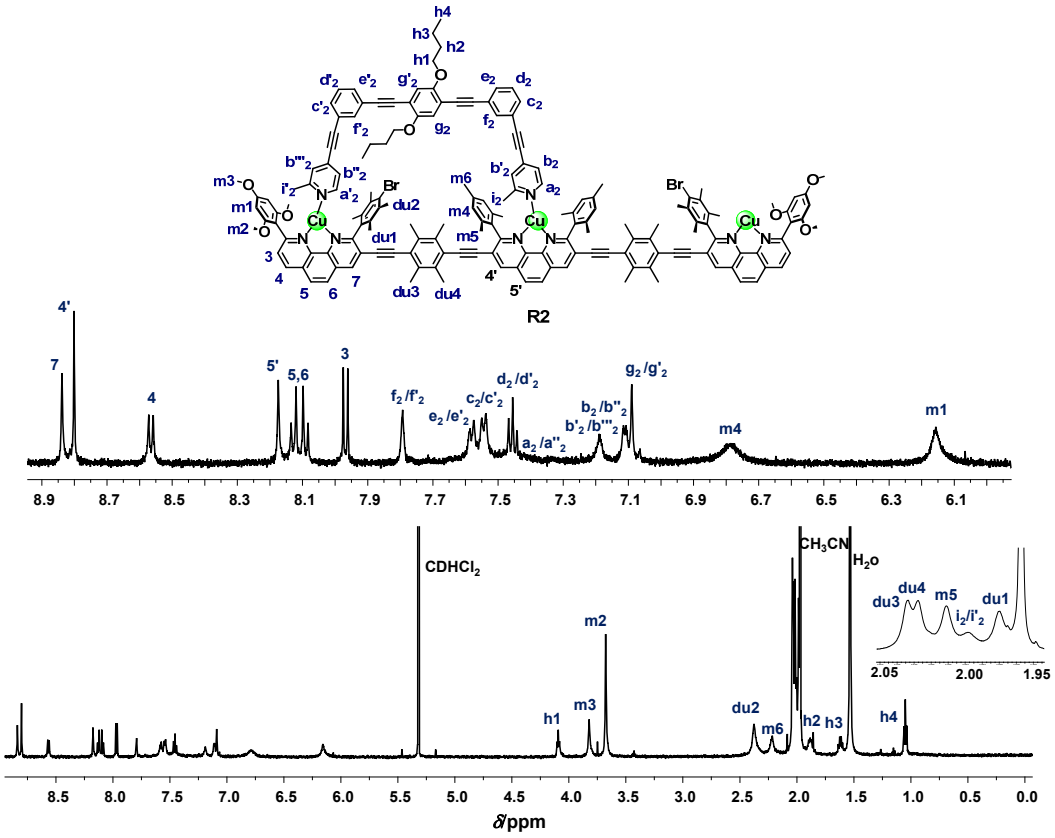

Figure S19. ^{1}H NMR spectrum (CD_2Cl_2, 600 MHz) of nanorotor **R2.**

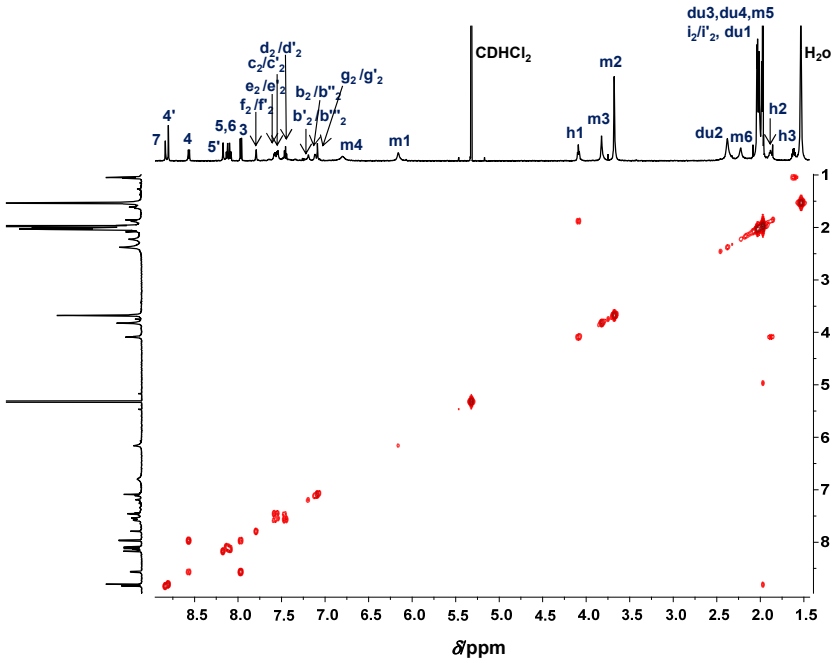

Figure S20. ^{1}H-^{1}H COSY NMR spectrum (CD_2Cl_2, 400 MHz) of nanorotor **R2**.

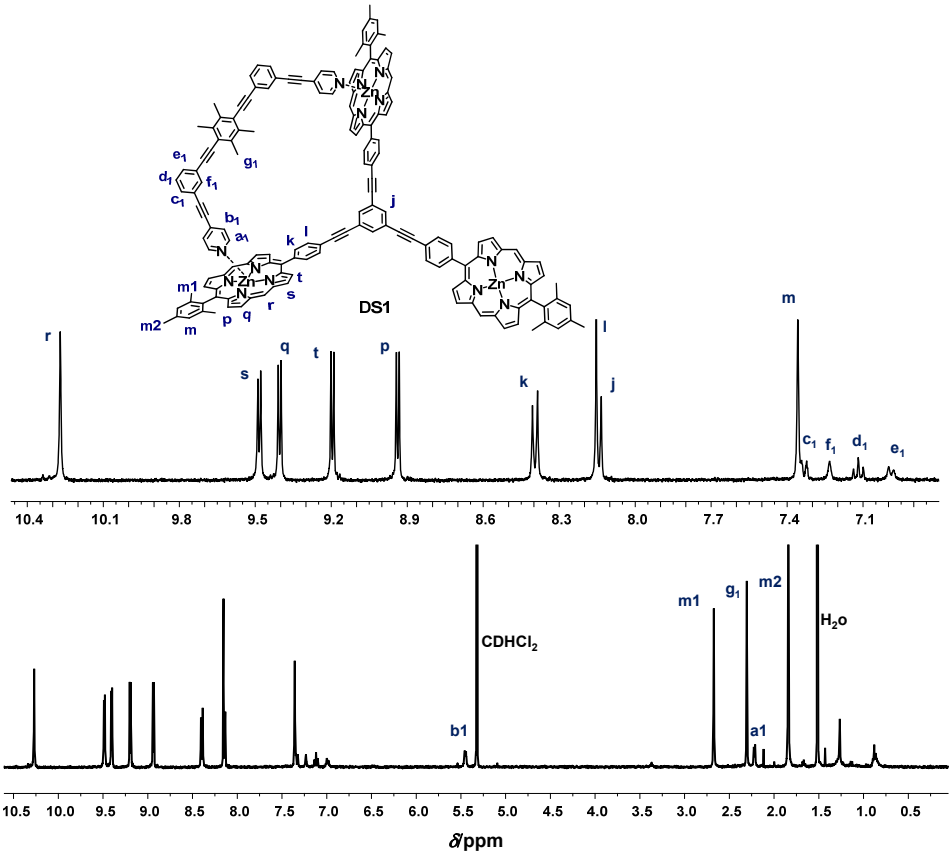

Figure S21. ^{1}H NMR spectrum (CD_2Cl_2, 400 MHz) of slider-on-deck **DS1.**

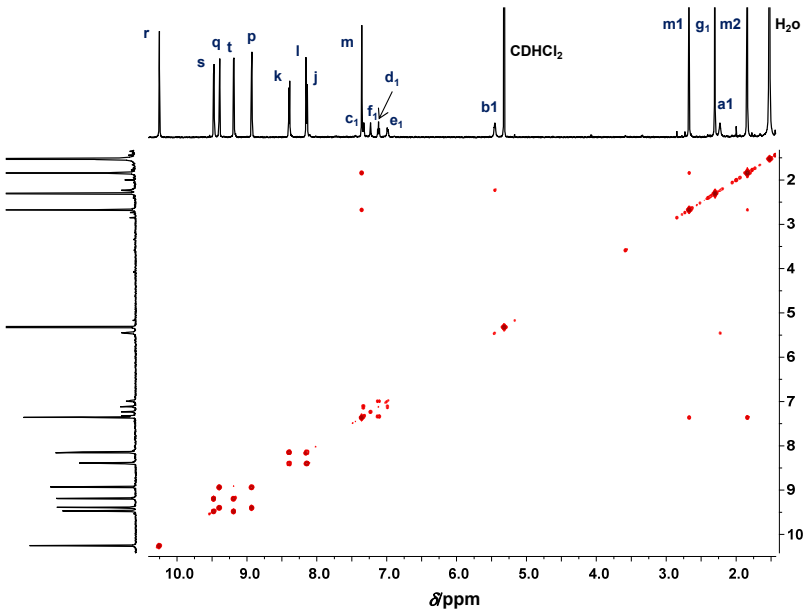

Figure S22. ^{1}H-^{1}H COSY NMR spectrum (CD_2Cl_2, 400 MHz) of slider-on-deck **DS1**.

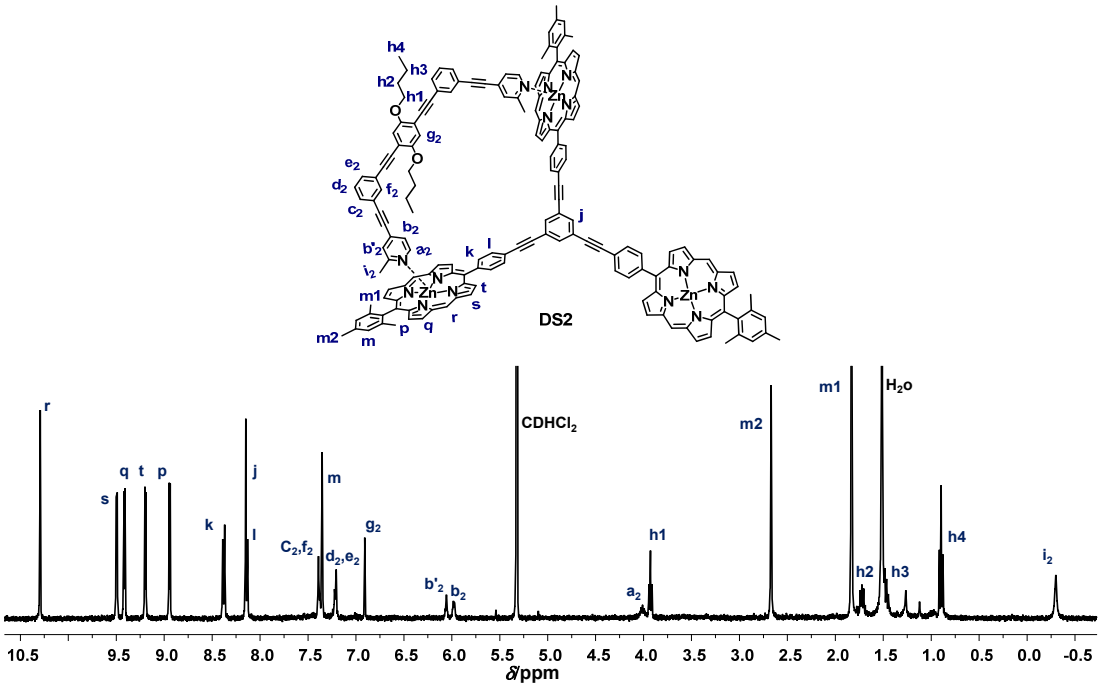

Figure S23. ^{1}H NMR spectrum (CD_2Cl_2, 400 MHz) of slider-on-deck **DS2.**

5. Comparison of NMR spectra.

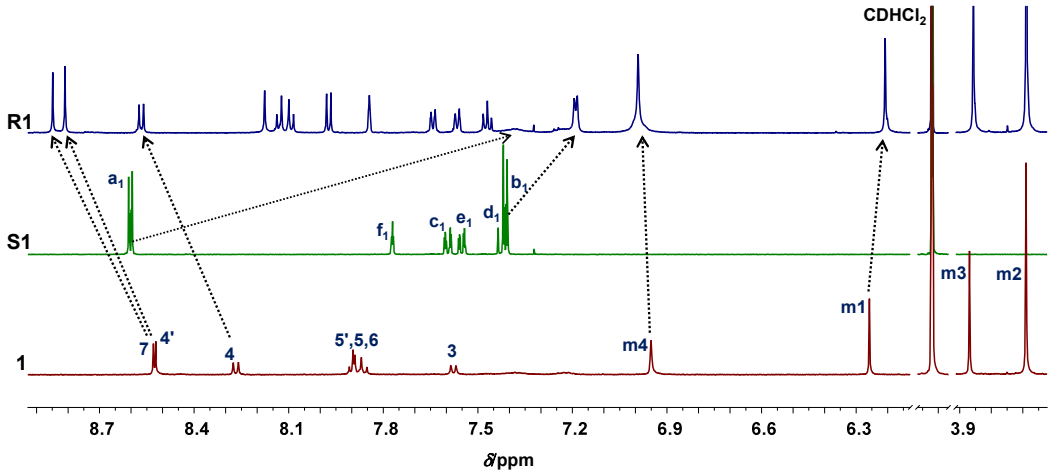

Figure S24. Partial ^{1}H NMR spectra (400 MHz, CD_2Cl_2, 298 K) of **1, S1** and **R1**.

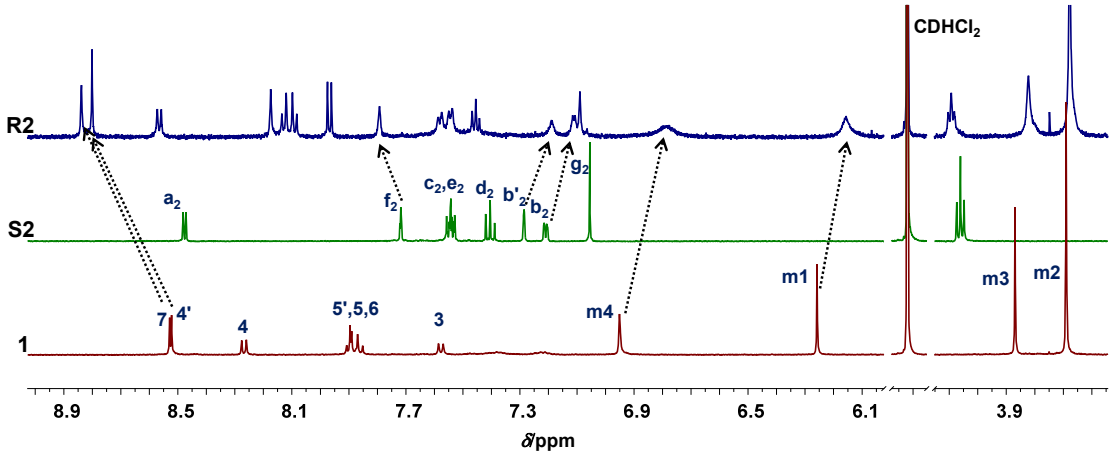

Figure S25. Partial ^{1}H NMR spectra (400 MHz, CD_2Cl_2, 298 K) of **1, S2** and **R2**.

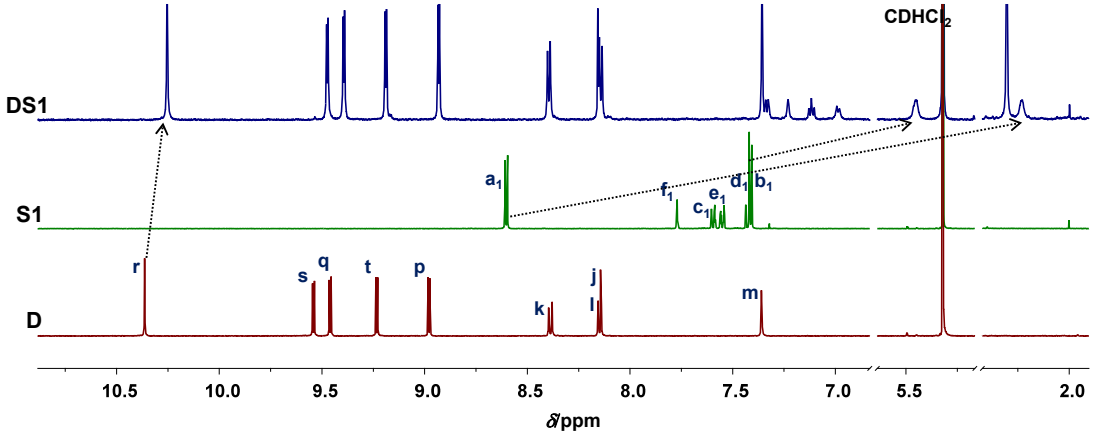

Figure S26. Partial ^{1}H NMR spectra (400 MHz, CD_2Cl_2, 298 K) of **D, S1** and **DS1**.

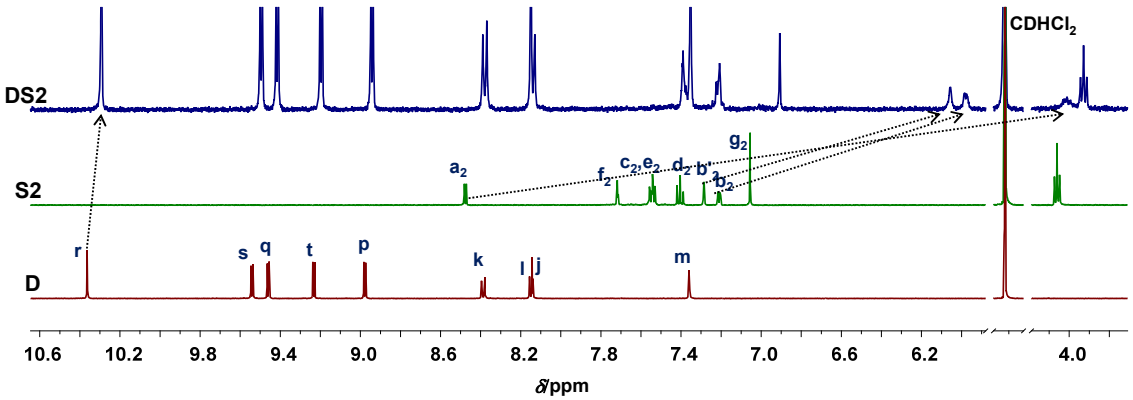

Figure S27. Partial ^{1}H NMR spectra (400 MHz, CD_2Cl_2, 298 K) of **D, S2** and **DS2**.

6. DOSY NMR spectra

Calculation of hydrodynamic radius. The diffusion coefficient *D* for **R1**, **R2**, **DS1** and **DS2** were obtained from their DOSY spectrum. The corresponding hydrodynamic radius *r* was calculated by using the Stokes Einstein equation

$$r = k_B T/6\pi\eta D$$

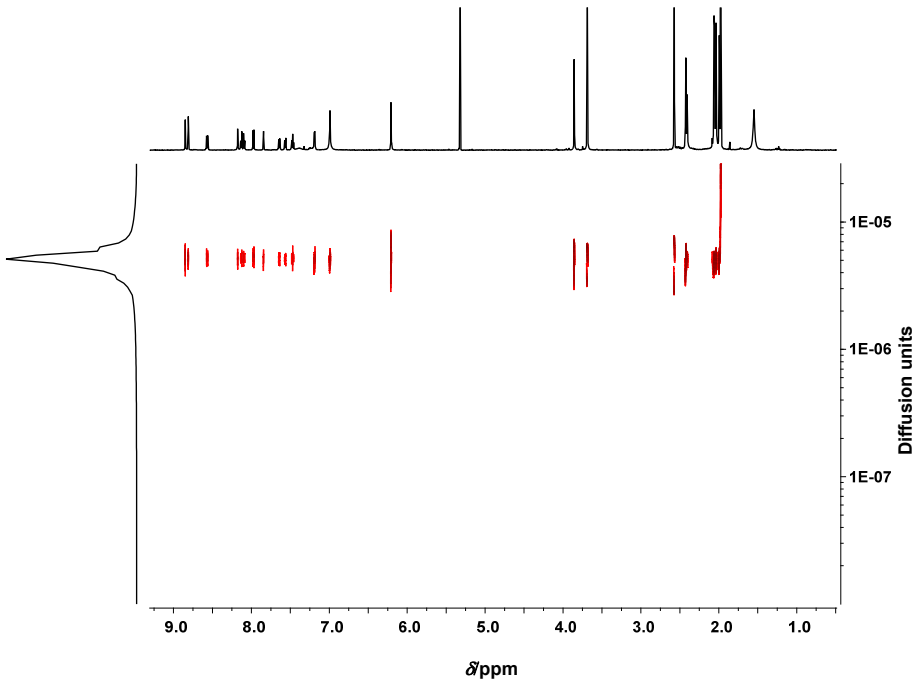

Figure S28. DOSY NMR of **R1** in CD_2Cl_2 (600 MHz, 298 K). Diffusion coefficient $D = 3.8 \times 10^{-10}$ m^2 s^{-1}, hydrodynamic radius $r = 14.0$ Å.

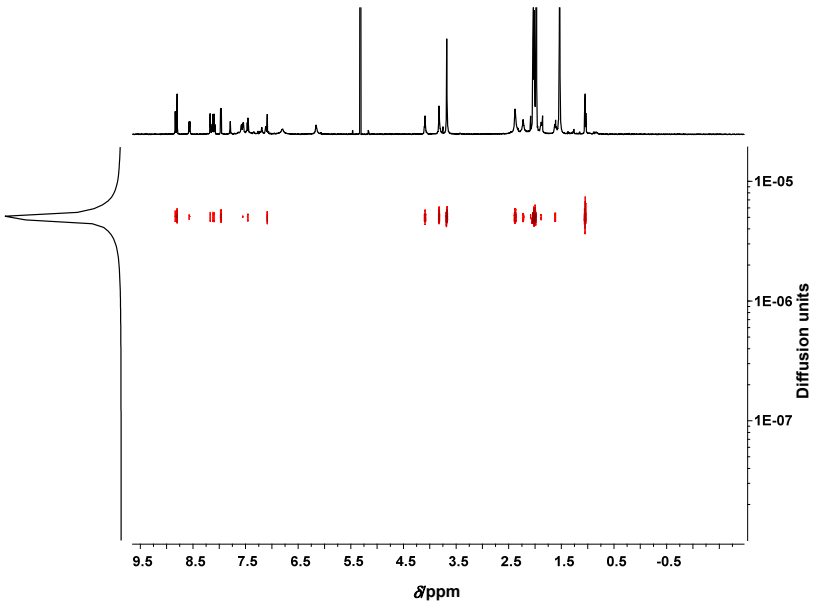

Figure S29. DOSY NMR of **R2** in CD_2Cl_2 (600 MHz, 298 K). Diffusion coefficient $D = 3.5 \times 10^{-10}$ m^2 s^{-1}, hydrodynamic radius $r = 15.2$ Å.

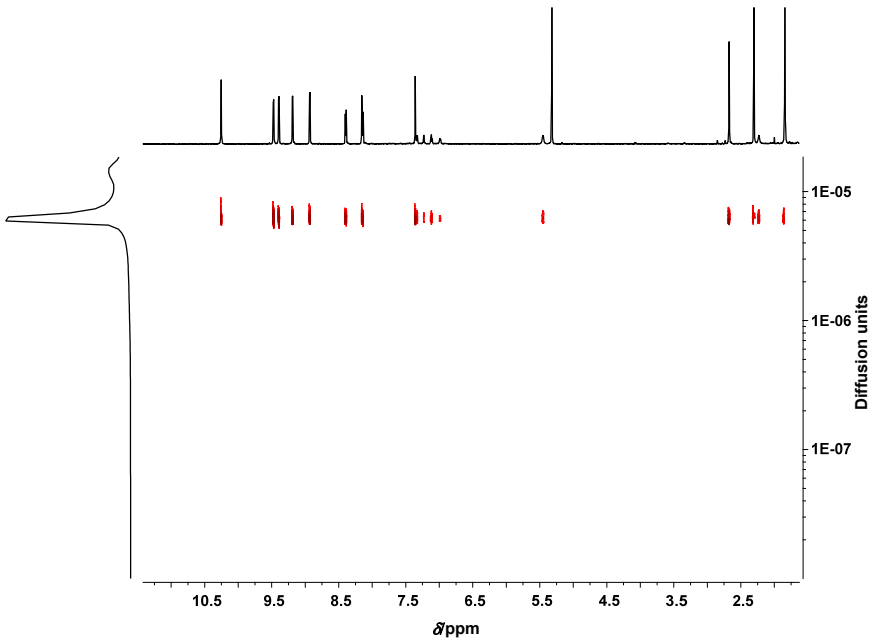

Figure S30. DOSY NMR of **DS1** in CD_2Cl_2 (600 MHz, 298 K). Diffusion coefficient $D = 4.4 \times 10^{-10}$ m^2 s^{-1}, hydrodynamic radius $r = 12.1$ Å.

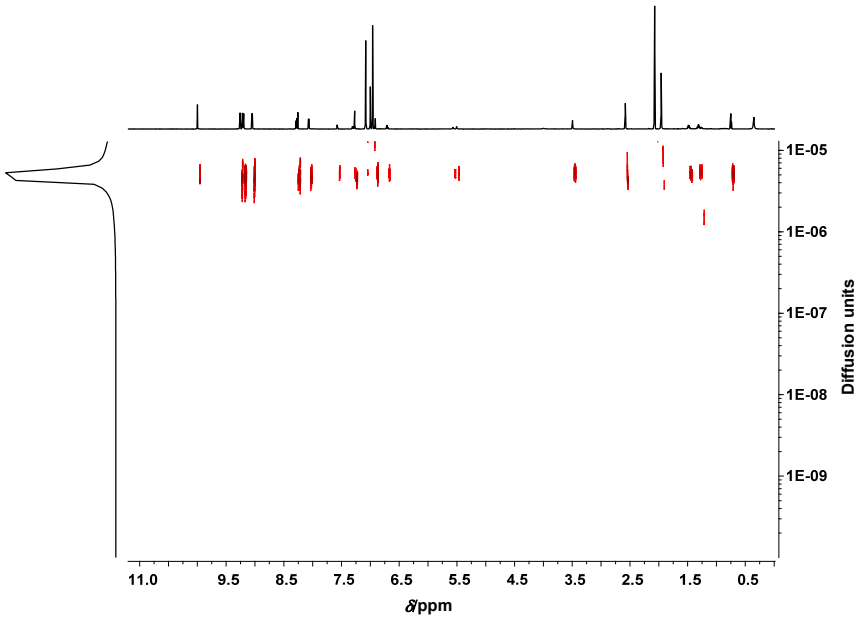

Figure S31. DOSY NMR of **DS2** in toluene-d_8 (600 MHz, 298 K). Diffusion coefficient $D = 2.7 \times 10^{-10}$ m^2 s^{-1}, hydrodynamic radius $r = 13.7$ Å.

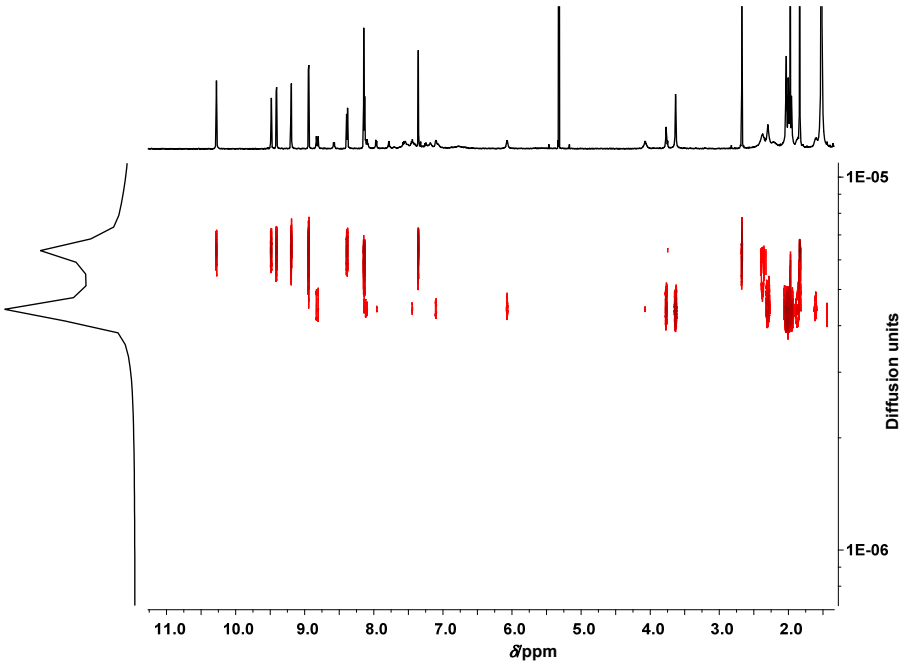

Figure S32. DOSY NMR of the final mixture after metathesis in CD_2Cl_2 (600 MHz, 298 K). Diffusion coefficient for **DS1** [$D = 4.6 \times 10^{-10}$ m^2 s^{-1}, hydrodynamic radius $r = 11.6$ Å] and **R2** [$D = 3.3 \times 10^{-10}$ m^2 s^{-1}, hydrodynamic radius $r = 16.1$ Å].

7. ESI-MS spectra

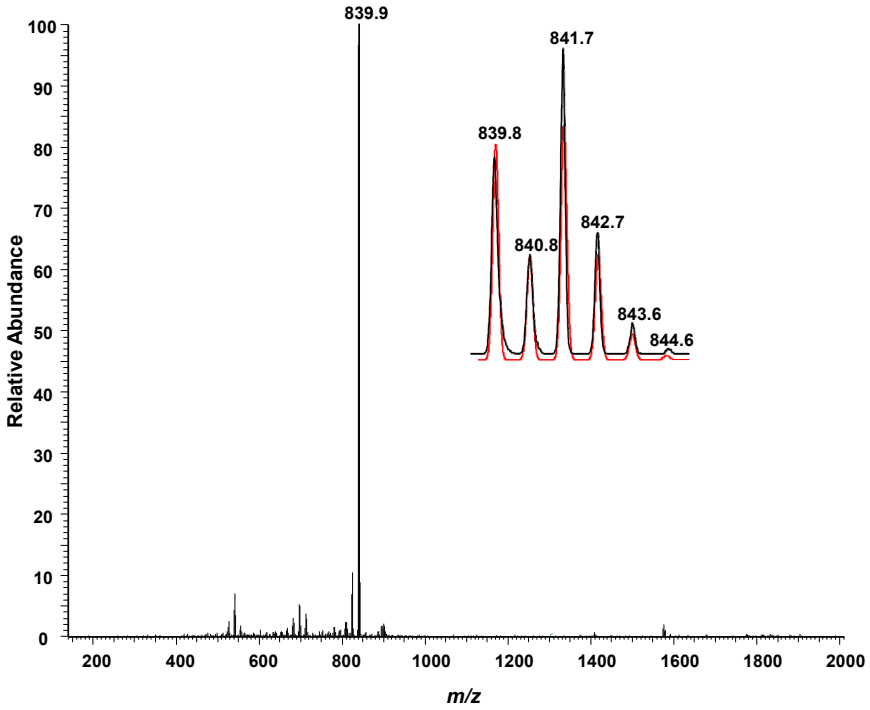

Figure S33. ESI-MS of **8** in CH_2Cl_2.

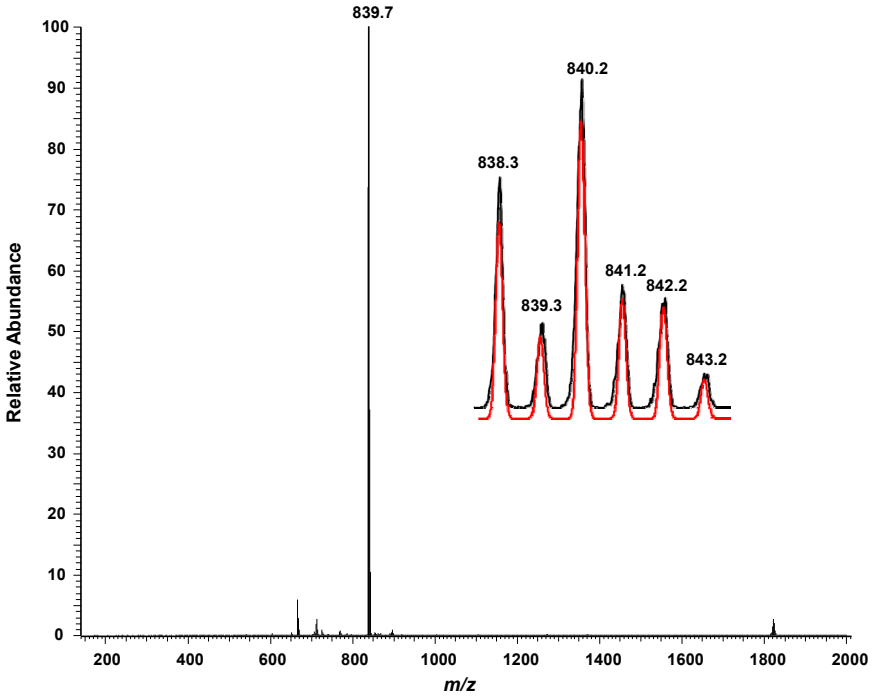

Figure S34. ESI-MS of **C2** in CH_2Cl_2.

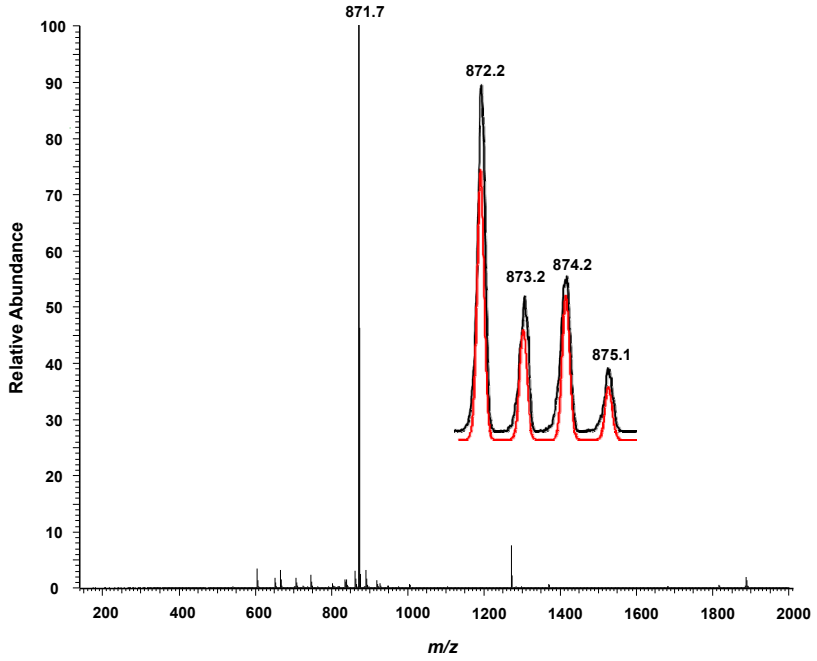

Figure S35. ESI-MS of **C4** in CH_2Cl_2.

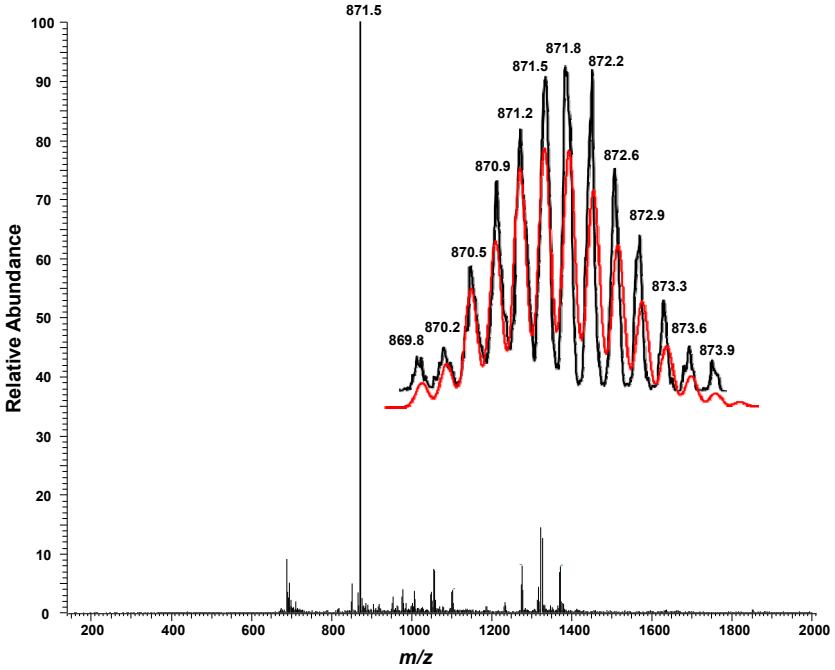

Figure S36. ESI-MS of **R1** in CH_2Cl_2.

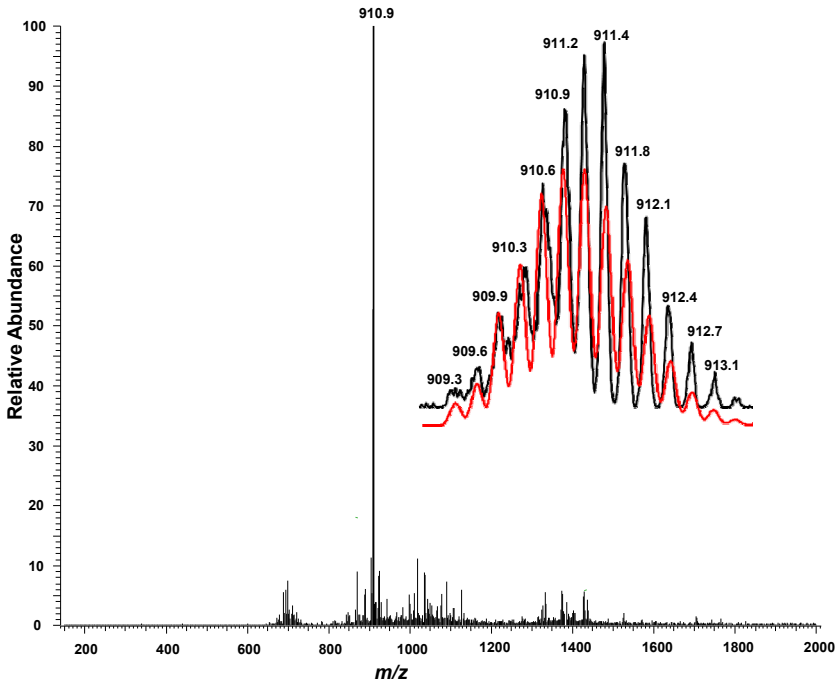

Figure S37. ESI-MS of **R2** in CH_2Cl_2.

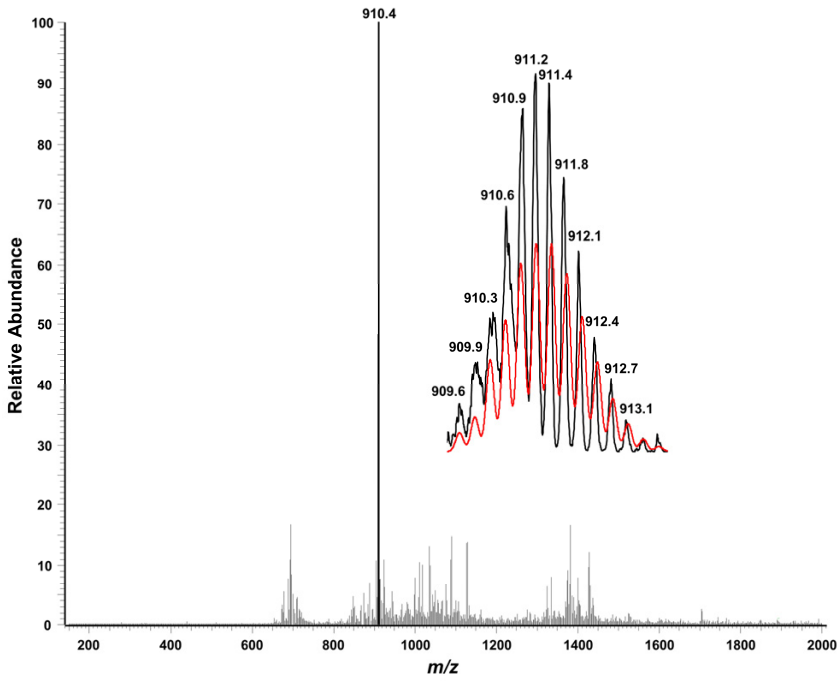

Figure S38. ESI-MS of **DS1** and **R2** formed after metathesis. **DS1** is ESI-MS silent (CH_2Cl_2).

8. Variable temperature studies and determination of kinetic parameters

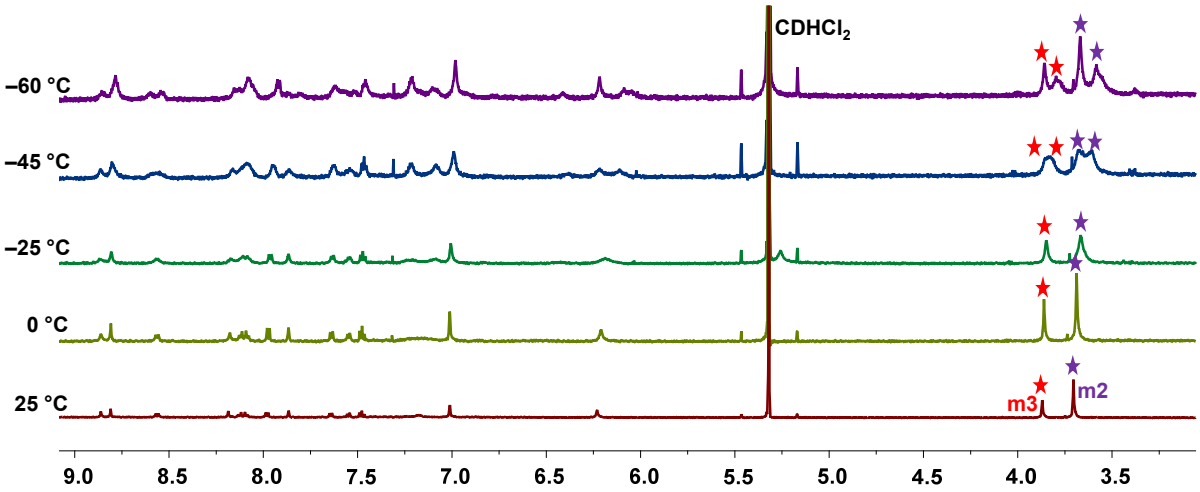

Figure S39. Partial ^{1}H VT-NMR (CD_2Cl_2, 600 MHz) of **R1** showing the splitting of proton m3-H (red asterisk marked) and m2-H (violet asterisk marked).

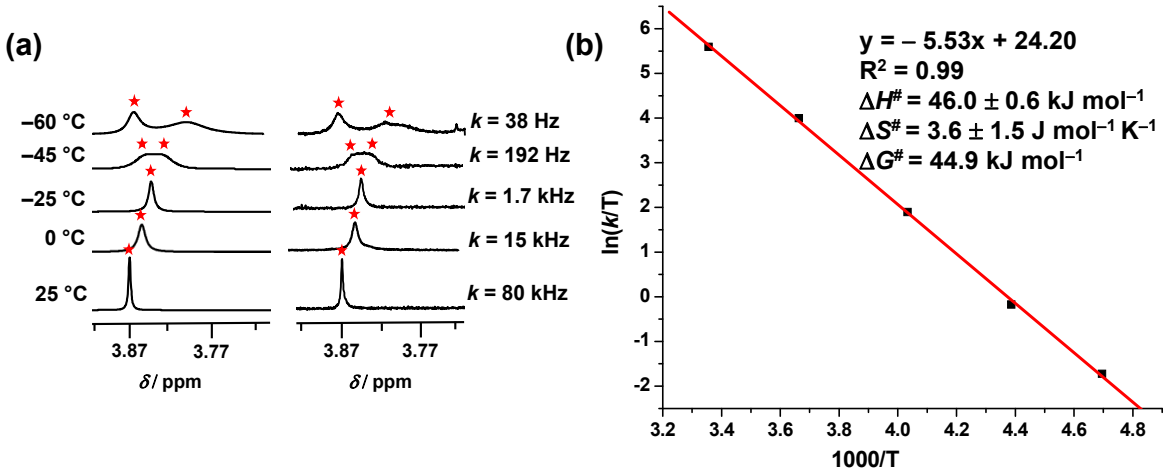

Figure S40. (a) Simulated and experimental ^{1}H VT-NMR (CD_2Cl_2, 600 MHz) of **R1** shows the splitting of m3-H (red asterisk marked) and (b) Eyring plot for rotational exchange in **R1.**

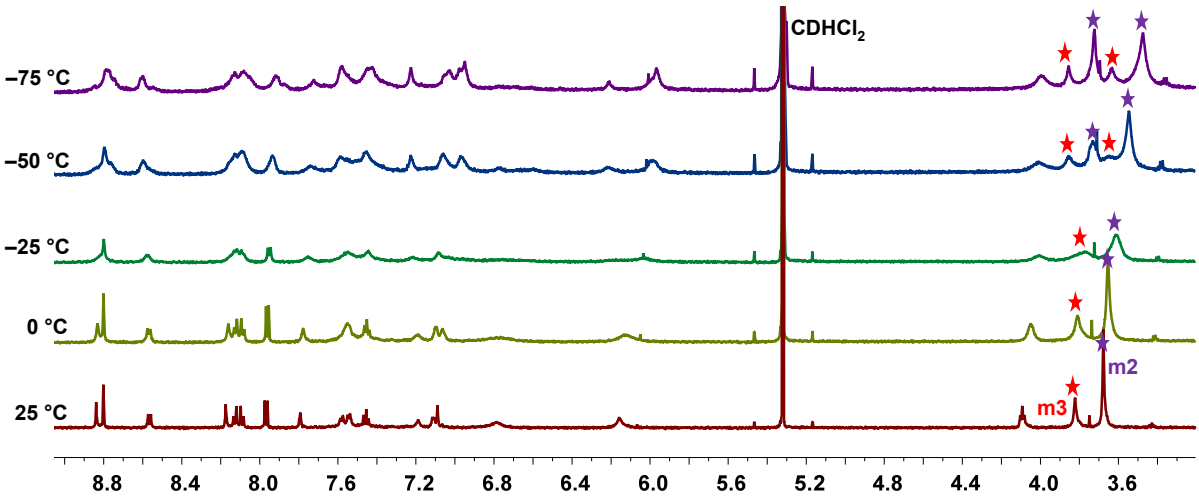

Figure S41. Partial ^{1}H VT-NMR (CD_2Cl_2, 600 MHz) of **R2** showing the splitting of proton m3-H (red asterisk marked) and m2-H (violet asterisk marked).

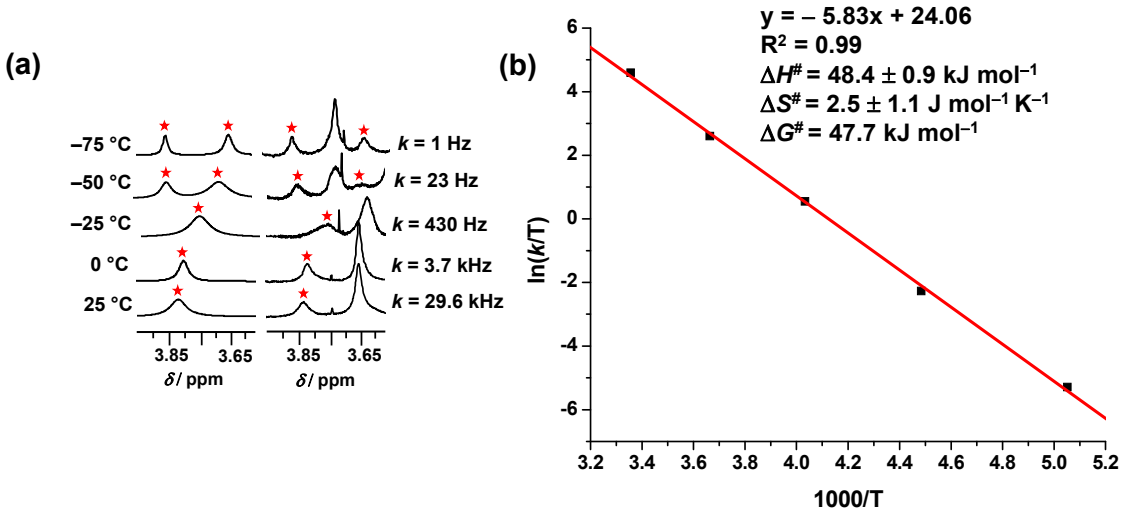

Figure S42. (a) Simulated and experimental ^{1}H VT-NMR (CD_2Cl_2, 600 MHz) of **R2** shows the splitting of m3-H (red asterisk marked) and (b) Eyring plot for rotational exchange in **R2.**

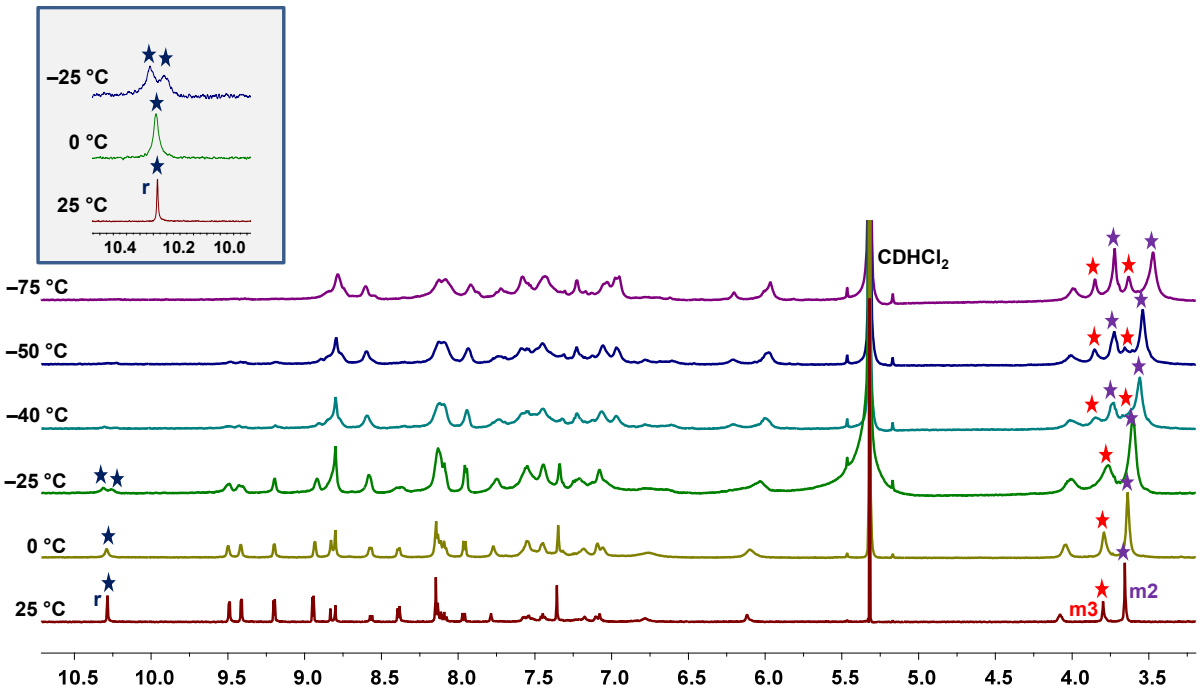

Figure S43. Partial ^{1}H VT-NMR (CD_2Cl_2, 600 MHz) of **DS1** and **R2** formed by metathesis showing the splitting of proton r-H (blue asterisk marked) of **DS1** and m3-H (red asterisk marked), m2-H (violet asterisk marked) of **R2**.

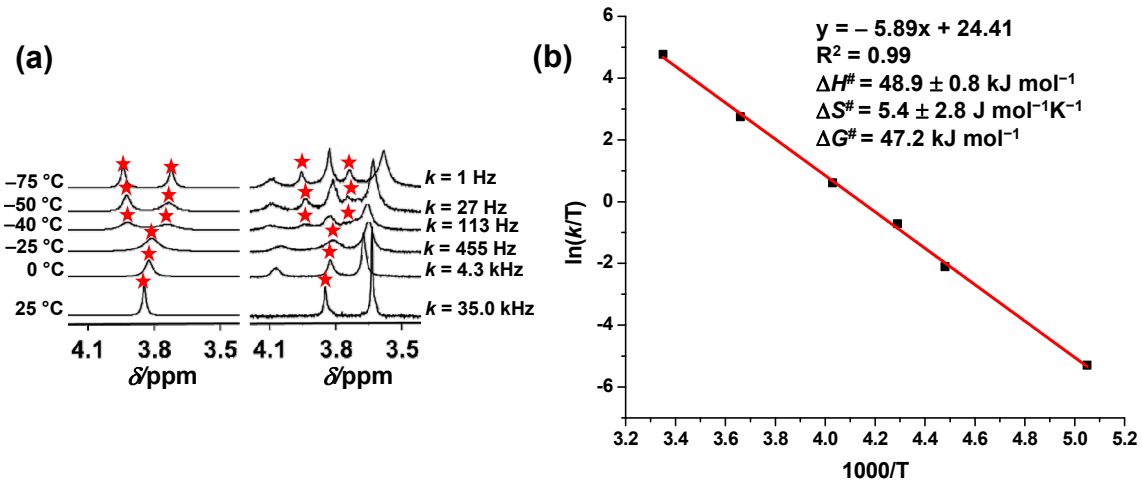

Figure S44. (a) Simulated and experimental ^{1}H VT-NMR (CD_2Cl_2, 600 MHz) of **R2** (formed in metathesis reaction together with **DS1**) shows the splitting of m3-H (red asterisk marked) and (b) Eyring plot for rotational exchange in **R2 (**after metathesis**).**

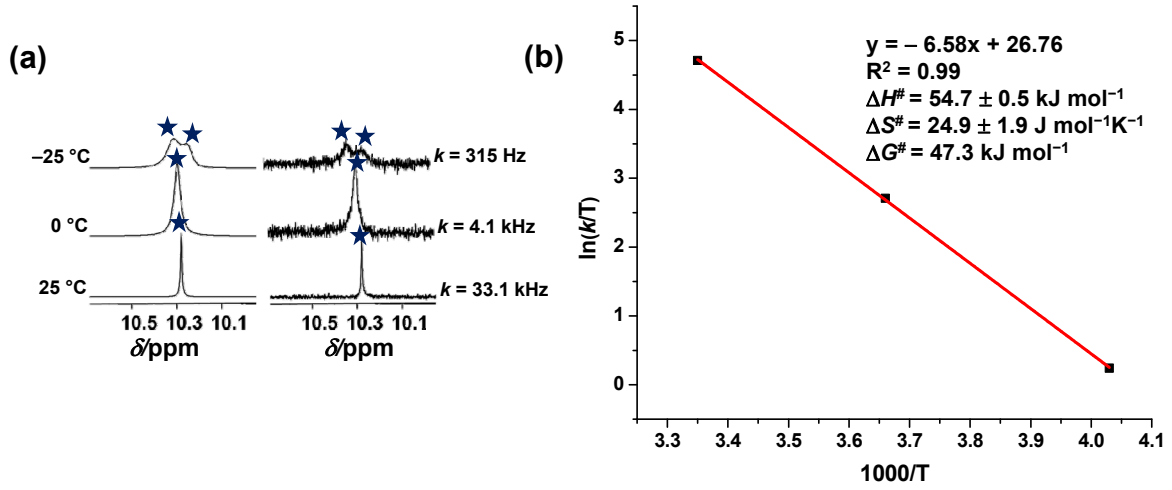

Figure S45. (a) Simulated and experimental ^{1}H VT-NMR (CD_2Cl_2, 600 MHz) of **DS1** (formed in metathesis reaction together with **R1**) shows the splitting of r-H (blue asterisk marked) and (b) Eyring plot for rotational exchange in **DS1 (**after metathesis**).**

Dynamic assembly	k_{298} / s^{-1}	$\Delta G_{298}^{\ddagger}$ / kJ mol^{-1}	$\Delta H^{\ddagger}$ / kJ mol^{-1}	$\Delta S^{\ddagger}$ / J mol^{-1} K^{-1}
R1	80000	44.9 ± 0.2	46.0 ± 0.6	3.6 ± 1.5
R2	29600	47.7 ± 0.6	48.5 ± 0.9	2.5 ± 1.1
DS1	32200	47.3 ± 0.2	54.7 ± 0.5	24.8 ± 2.2
DS2	440000	40.7 ± 0.2	42.9 ± 0.6	7.5 ± 2.5
R2 (mixture)	35000	47.2 ± 0.1	48.9 ± 0.8	5.4 ± 2.8
DS1 (mixture)	33100	47.3 ± 0.1	54.7 ± 0.5	24.9 ± 1.9

Figure S46. Experimental exchange frequency *k* at 25 °C and activation parameters of **R1**, **R2**, **DS1** and **DS2.**

9. Measurements of binding constants

a). Determination of log *K* of complex C2.

A UV-vis titration was performed to measure the binding constants between Cu^{+}-loaded **3** and **4**. A solution of $[Cu(\mathbf{3})]^{+}$ (9.5×10^{-6} M) was titrated with a 10^{-3} M solution of **4** in dichloromethane. The UV-vis response was analyzed by nonlinear curve-fitting. ΔA values were monitored at 271 nm. The following equation[6] was used for the fitting,

$$\Delta A = L*((K*(P+x)+1)-SQRT(((K*(P+x)+1)\text{^}2)-4*K*K*P*x))/(2*K*P).$$

With x and P representing $[Guest]_{total}$ and $[Host]_{total}$, respectively; L denoting ΔA at 100% complexation; L and K are parameters.

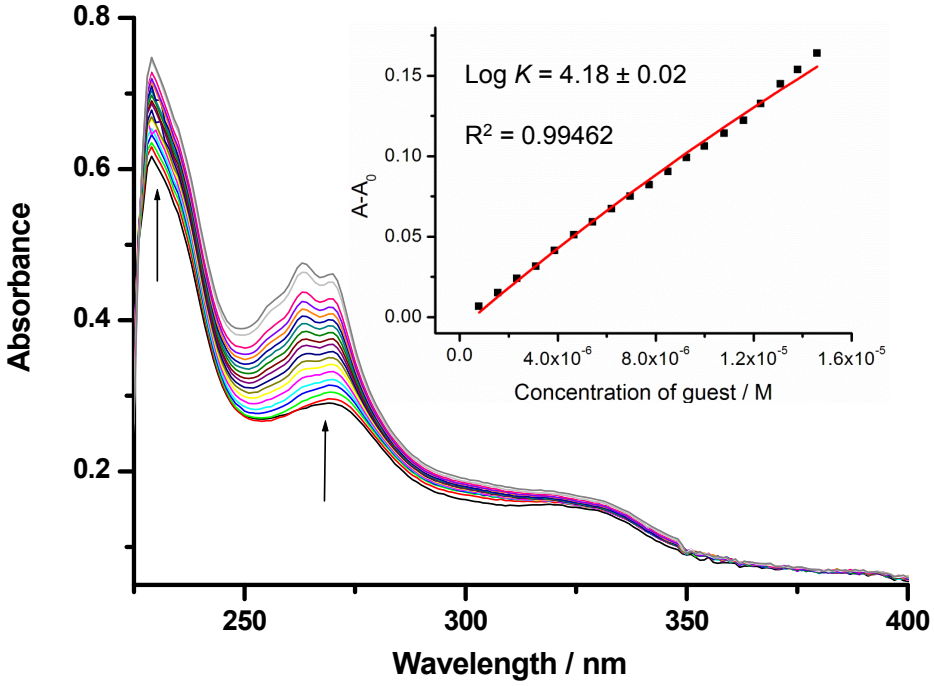

Figure S47. UV-vis titration of Cu^{+}-loaded **3** (9.5×10^{-6} M) with **4** (1×10^{-3} M). Inset: Fitting curve for binding constant determination.

b). Determination of log *K* of complex C4.

A UV-vis titration was performed to measure the binding constants between Cu^{+}-loaded **3** and **5**. A solution of $[Cu(\mathbf{3})]^{+}$ (9.5×10^{-6} M) was titrated with a 5.7×10^{-4} M solution of **5** in dichloromethane. The UV-vis results were analyzed by nonlinear curve-fitting. ΔA values were monitored at 271 nm. The above mentioned equation was used for the fitting.

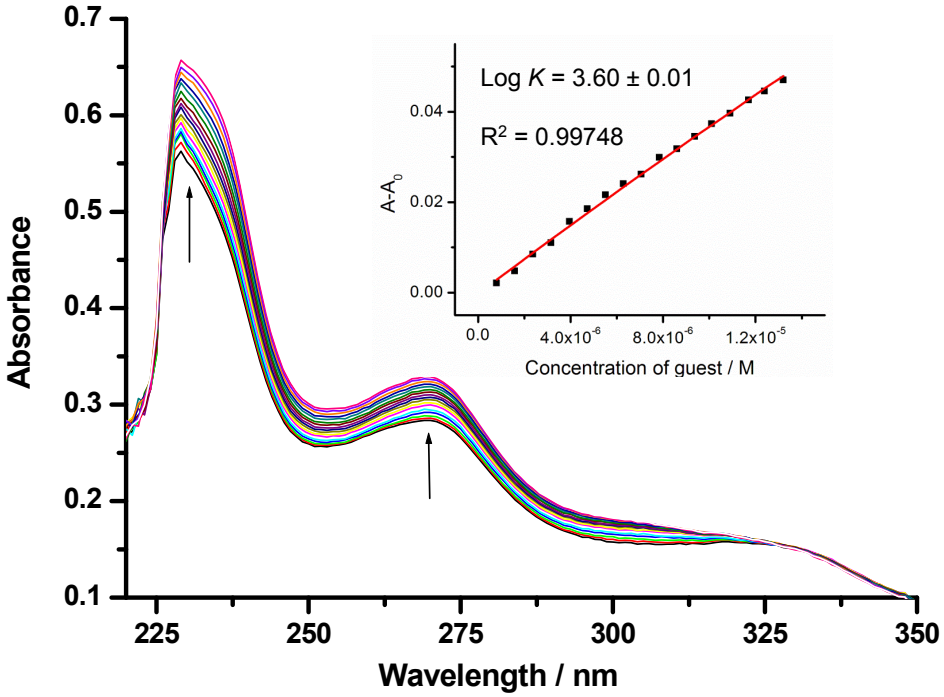

Figure S48. UV-vis titration of Cu^{+}-loaded **3** (9.5×10^{-6} M) with **5** (5.7×10^{-4} M). Inset: Fitting curve for binding constant determination.

10. UV-vis spectra

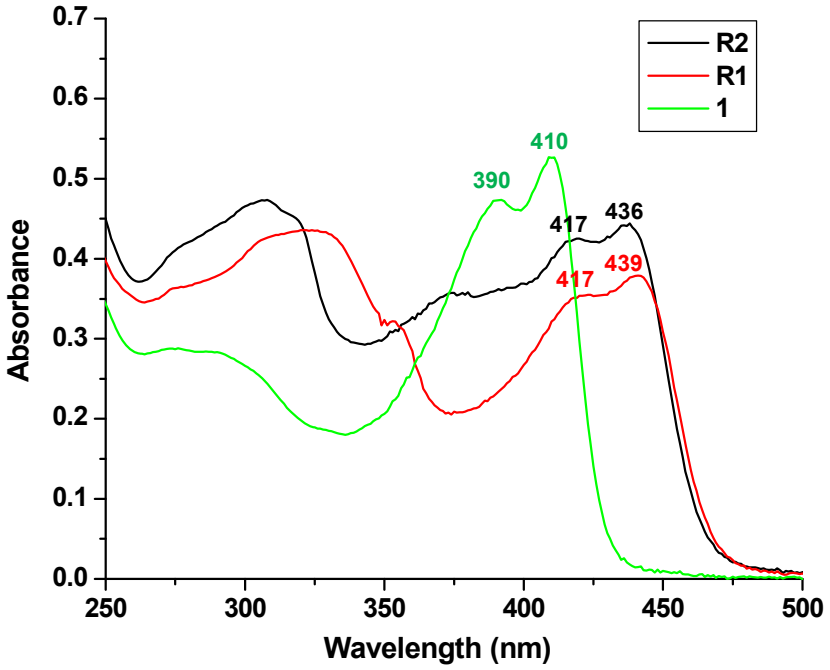

Figure S49. UV-vis spectra of **1, R1** and **R2** (3.6×10^{-6} M) in CH_2Cl_2 at 298 K.

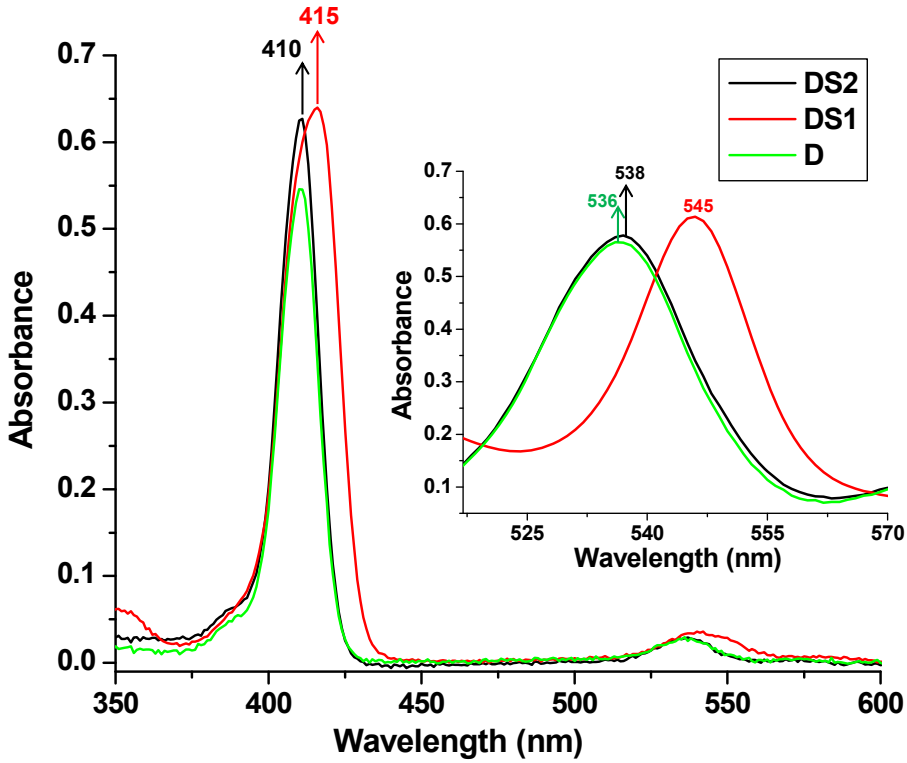

Figure S50. Full UV-vis spectra of **D**, **DS1** and **DS2** (1×10^{-6} M) in CH_2Cl_2 at 298 K. Insert: Q band of **D**, **DS1** and **DS2** (to monitor it we have used a concentrated (1×10^{-5} M) solution).

11. Kinetics of metathesis

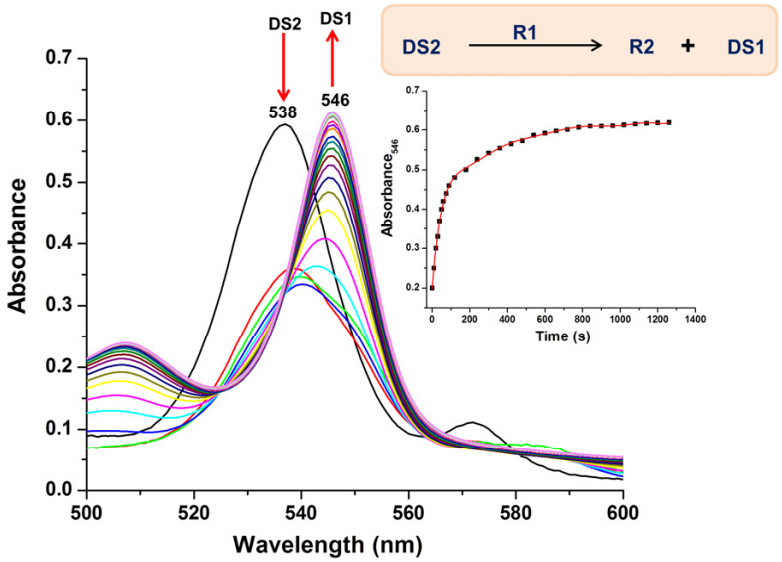

Figure S51. UV-vis spectra of the reaction between **DS2** and **R1** at 298 K in CH_2Cl_2 indicating formation of **DS1**. Inset: Change of absorbance at λ = 546 nm with time (v_o = 1.31 × 10^{-7} mol $L^{-1}s^{-1}$).

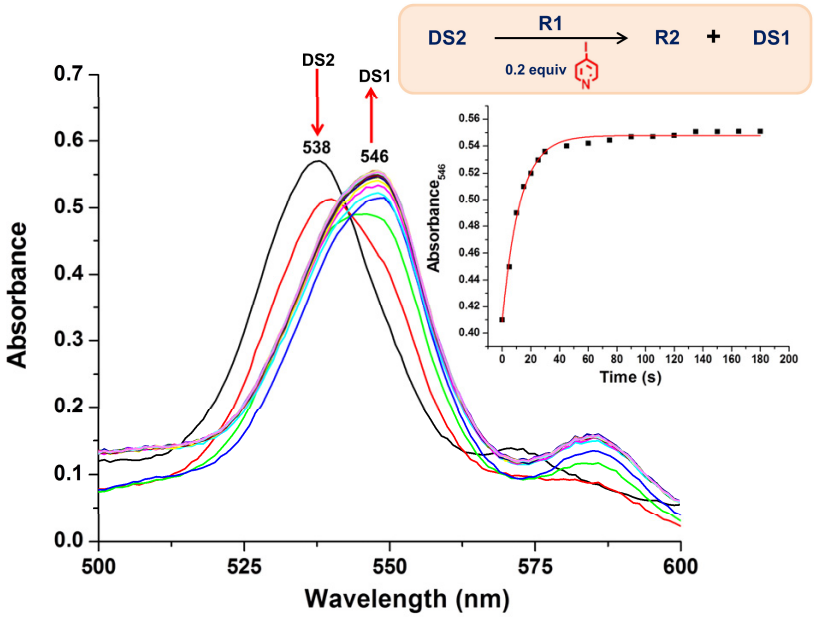

Figure S52. UV-vis spectra of the reaction between **DS2** and **R1** at 298 K in CH_2Cl_2 in presence of 4-iodopyridine (20 mol%). Inset: Change of absorbance at λ = 546 nm with time (v_o = 1.40 × 10^{-6} mol $L^{-1}s^{-1}$).

12. References

1. Samanta, D.; Paul, I.; Schmittel, M. *Chem. Commun*. **2017**, *53*, 9709.

2. Goswami, A.; Paul, I.; Schmittel, M. *Chem*. *Commun*. **2017**, *53*, 5186-5189.

3. Richelle, G. J. J.; Ori, S.; Hiemstra, H.; Maarseveen, J. H. V.; Timmerman, P. *Angew. Chem. Int. Ed.* **2018**, *57*, 501.

4. Schmittel, M.; Michel, C.; Wiegrefe, A. *Synthesis* **2005**, *3*, 1561.

5. Paul, I.; Goswami, A.; Mittal, N.; Schmittel, M. *Angew. Chem. Int. Ed*. **2018**, *57*, 354.

6. Hristova, Y. R.; Smulders, M. J.; Clegg, J. K.; Breiner, B.; Nitschke, J. R.; *Chem. Sci.* **2011**, *2*, 638.